



CASE FILE
COPY

REPORT No. 83

WIND TUNNEL STUDIES
IN AERODYNAMIC PHENOMENA
AT HIGH SPEED



NATIONAL ADVISORY COMMITTEE
FOR AERONAUTICS

THIS DOCUMENT IS IN THE FILES OF
NATIONAL ADVISORY COMMITTEE FOR AERONAUTICS
LANGLEY RESEARCH AIRFIELD
LANGLEY, VIRGINIA
UNCLASSIFIED
AS FOLLOWS:
NATIONAL ADVISORY COMMITTEE FOR AERONAUTICS
1720 AVENUE OF THE STARS
WASHINGTON 26, D.C.



WASHINGTON
GOVERNMENT PRINTING OFFICE
1920

REPORT No. 83

WIND TUNNEL STUDIES
IN AERODYNAMIC PHENOMENA
AT HIGH SPEED



NATIONAL ADVISORY COMMITTEE
FOR AERONAUTICS



WASHINGTON
GOVERNMENT PRINTING OFFICE
1920

REPORT No. 83

WIND TUNNEL STUDIES
IN AERODYNAMIC PHENOMENA
AT HIGH SPEED

NATIONAL ADVISORY COMMITTEE
FOR AERONAUTICS



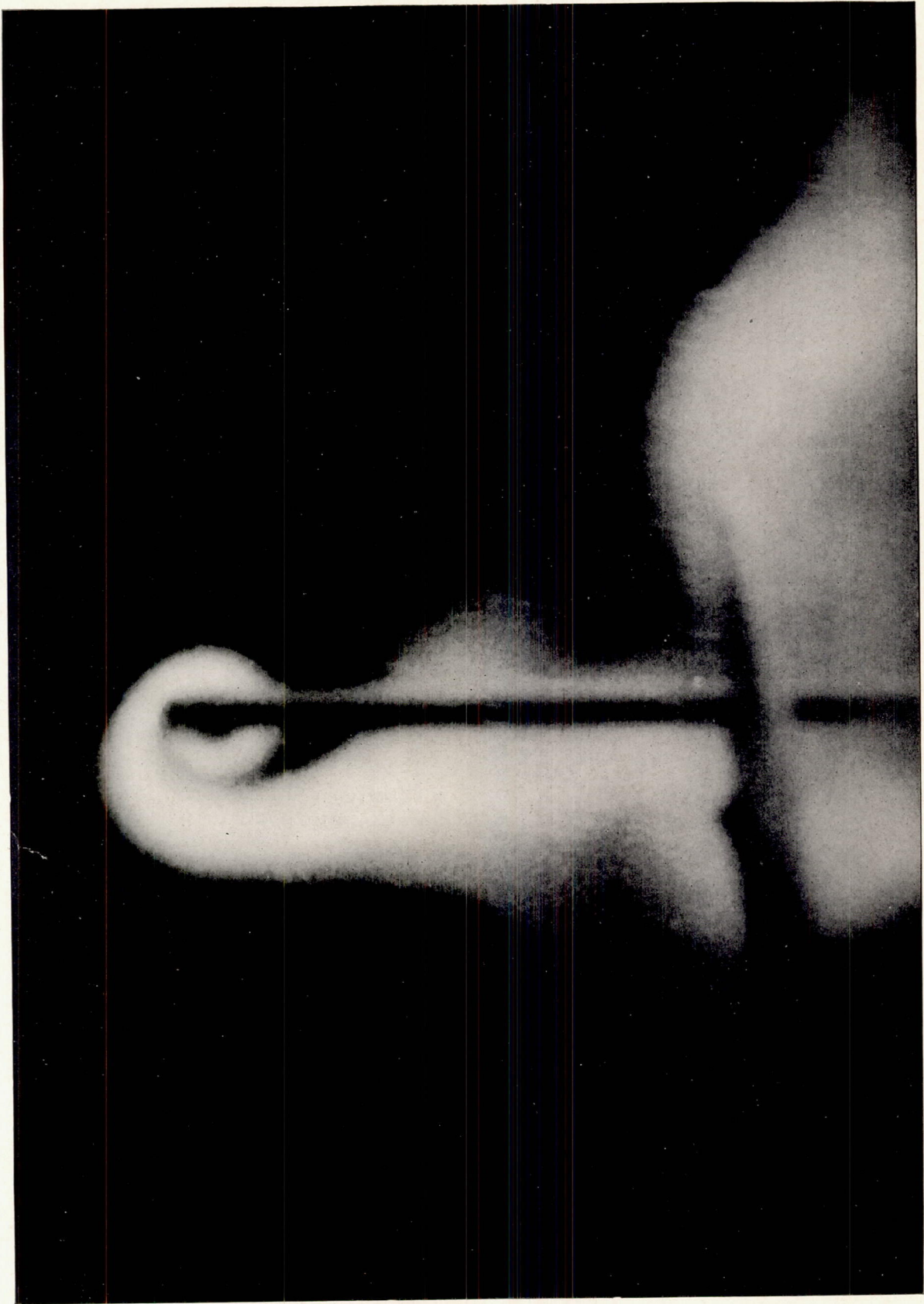
WASHINGTON
GOVERNMENT PRINTING OFFICE
1936

REPORT No. 83

**WIND TUNNEL STUDIES IN AERODYNAMIC PHENOMENA
AT HIGH SPEED**

- PART 1. MODEL WIND TUNNEL EXPERIMENTS
PART 2. THE McCOOK FIELD WIND TUNNEL
PART 3. MODEL TESTS ON PROPELLER AEROFOILS**

By F. W. CALDWELL and E. N. FALES
Engineering Division, Air Service of the Army, McCook Field, Dayton, Ohio



TIP VORTEX ON MODEL AEROFOIL.

REPORT NO. 83.

PART I.

MODEL WIND TUNNEL EXPERIMENTS.

By F. W. CALDWELL and E. N. FALES.

INTRODUCTION.

This report was prepared for publication by the National Advisory Committee for Aeronautics by Messrs. F. W. Caldwell and E. N. Fales of the Engineering Division, Air Service of the Army, McCook Field, Dayton, Ohio, with the approval of Col. T. H. Bane, U. S. Army, Chief of the Engineering Division and Member of the National Advisory Committee for Aeronautics.

A great amount of research and experimental work has been done, and fair success attained, in an effort to place airplane and propeller design upon an empirical basis. One can not, however, fail to be impressed with the lack of data available toward establishing flight phenomena upon a rational basis, such that they may be interpreted in terms of the laws of physics. Almost the whole field of aeronautical experiment and design is based on the law of dynamic similarity.

In practical work it has been necessary to combine the results of model tests with empirical factors which are certainly limited in their application. The writers see no reason whatever for skepticism about the application of the law of dynamic similarity provided we really have similarity. It is certainly insufficient, however, to have geometrical similarity between the solid objects being studied. We must have in addition similarity of the character of the air flow.

Mathematical studies of first importance, which are now classical, on the nature of the flow about an aerofoil have been developed by Helmholtz, Kirchoff, Lord Rayleigh, Lanchester, Prandtl, Kutta, Karman, Greenhill, Lewis, and others. Dr. Georges de Bothezat has put forward some very interesting ideas about the effect of stresses in the fluid on the nature of the air flow, and he has consented to write a note on that subject at the end of this report.

It is Dr. de Bothezat's conception that the type of flow which establishes itself is governed by the stresses set up in the air passing the aerofoil. The unit stresses increase as the velocity rises. It is easy to conceive that a given type of flow is possible only so long as the shearing stress, developed in the fluid, does not exceed a certain magnitude which depends on the value of the viscosity coefficient.

When the stress reaches a certain critical value, two adjacent layers of air begin to slide past each other and the character of the flow is changed. Apparently such a change must bring with it a change of aerofoil characteristics since there is no longer flow similarity. This condition was actually encountered in most of the high speed tests referred to in this paper. The photograph of figure 2 shows the flow at a speed where such a change is incipient.

Experimental investigation of the flow has heretofore been rather unsuccessful because of lack of adequate methods. The writers laid out the design of the McCook Field wind tunnel to investigate the scaling effect due to the high velocity of propeller aerofoils. During the course of the experiments, however, it was found possible to visualize the air flow by means of the method described in Section II. This was made use of to study some changes in flow which affect the characteristics of the aerofoil in a very great degree.

The experiments were made under authority of Col. T. H. Bane, commanding officer of the field.

Acknowledgment is due the Bureau of Standards for furnishing laboratory facilities, and to Messrs. W. G. Gwynn and J. R. Randolph for carrying out the model wind-tunnel experiments. Acknowledgment is also due Messrs. C. P. Grimes, D. A. Dickey, and J. F. Piccard for assistance in carrying out the experiments at McCook Field.

The writers wish particularly, however, to express their appreciation of Prof. Gaetano Lanza, who in 1909-1912 assisted them in the researches which were a preliminary to those recorded in this paper. Prof. Lanza was at that time head of the mechanical engineering department at the Massachusetts Institute of Technology; he was the first active patron of aerodynamics on the staff of that institution, and prior to 1909, had erected a wind tunnel which became a stimulus to the authors' first aeronautical researches; he proposed a 12-foot wind tunnel for such work as early as 1910; and he put the entire shop and laboratory facilities of his department at the authors' disposal, for the wind tunnel, propeller, motor, and airplane material tests which were their major research subjects while students in his department.

OBJECT OF EXPERIMENTS.

The design of a wind tunnel differing from the usual type, especially with regard to large power and speed of flow, involves features whose suitability can not be predicted. After all available information has been secured on full size and model wind tunnels in various parts of the world, there remains much obscurity about the air-flow phenomena. The United States Army wind-tunnel designs, proposed as an item in the aircraft program of the recent war, have been developed toward the end of securing superior efficiency and steadiness of air flow. But it has been found that the conventional types fall short of the mark, and offer no precedent for many of the improvements conceived. Original experimentation has therefore become desirable for the purpose of comparing conventional and novel wind-tunnel arrangements.

DESCRIPTION OF APPARATUS.

The apparatus consisted of a one-twelfth scale model wind tunnel somewhat similar to the National Physical Laboratory type, but susceptible of a large number of variations. The "flue" was a sheet-iron cylinder 45 inches long by 8 inches diameter, provided at one end with a wooden intake bell and at the other with a 16° cone. For special tests the cone was modified at the large end either by constricting the discharge area, by affixing a 12-inch cylinder, by prolonging the cone, or by adding a large "vacuum chamber." Three types of intake were also tested.

The power plant consisted of a high-speed direct-current electric motor coupled to a long shaft, the whole properly mounted to avoid serious obstruction to the propeller discharge. The entire arrangement was adapted to the study of fan-cone arrangements, traverses in the flue, noise, etc. Five propellers were used comprising one 12-inch, 2-blade; two 12-inch, 4-blade; one 18-inch, 2-blade; one 18-inch, 4-blade. (Figs. 3, 4, 5.)

The conventional Pitot and impact tube apparatus was used for determining velocity, static, and dynamic heads. Flow lines were observed carefully by the smoke method and by the fine thread method.

METHOD OF TESTS.

The object of the tests was to compare specific arrangements of wind tunnels and to eliminate those proving inferior. It was therefore sufficient to establish relative rather than absolute efficiency in each test. While electrical power input was measured, it was found unnecessary to use the $\frac{\text{output}}{\text{input}}$ ratio as a means of interpreting the results; and the larger number of tests were made, not in terms of power, but in terms of a performance factor dependent on the effective pitch of the propeller blades.

A given set of tests, all made with the same fan, were then directly comparable with the others. The results have been represented graphically, in such a way as to show by diagrams the arrangement, the serial number, and the performance factor obtained in each test.

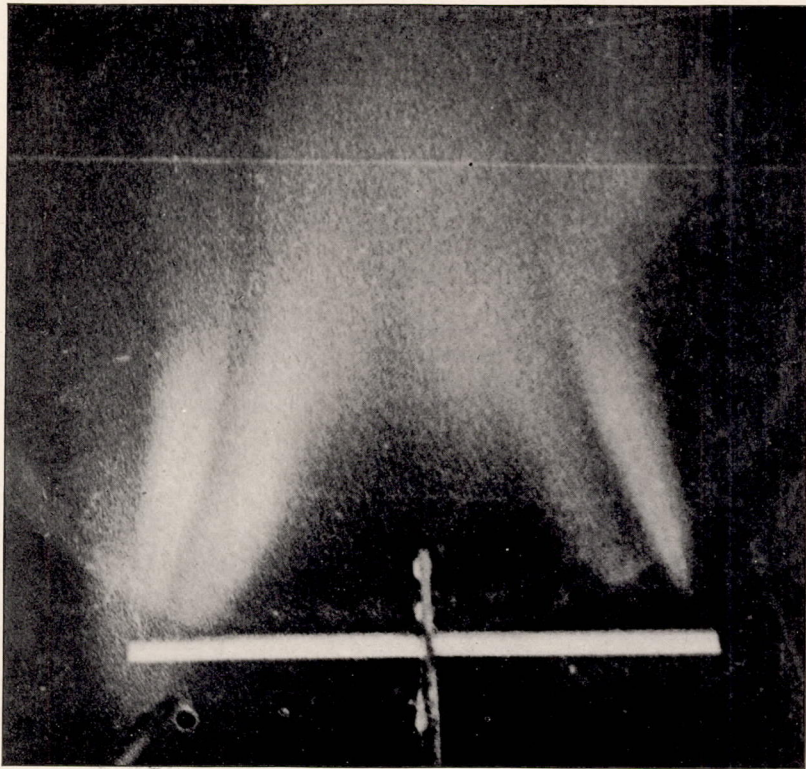


FIG. 1.—VIEW OF THE FLOW TAKEN FROM ABOVE THE MODEL.

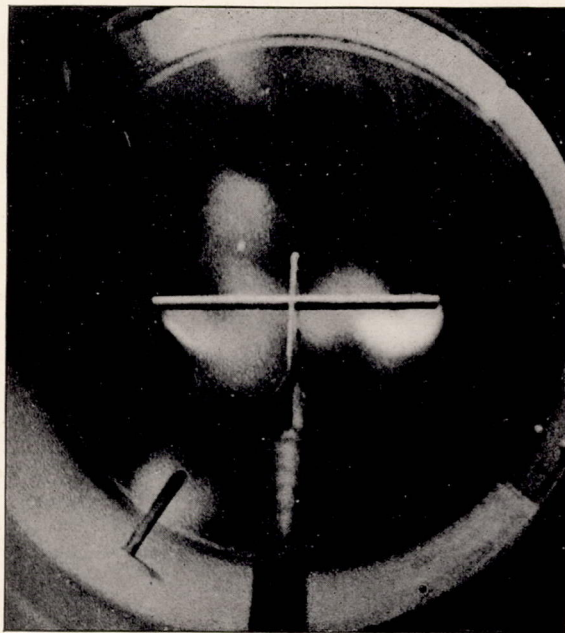


FIG. 2.—THE DISTURBED AIR BEHIND THE CENTER SUPPORT HAS HERE SHIFTED INTO THE LEFT.

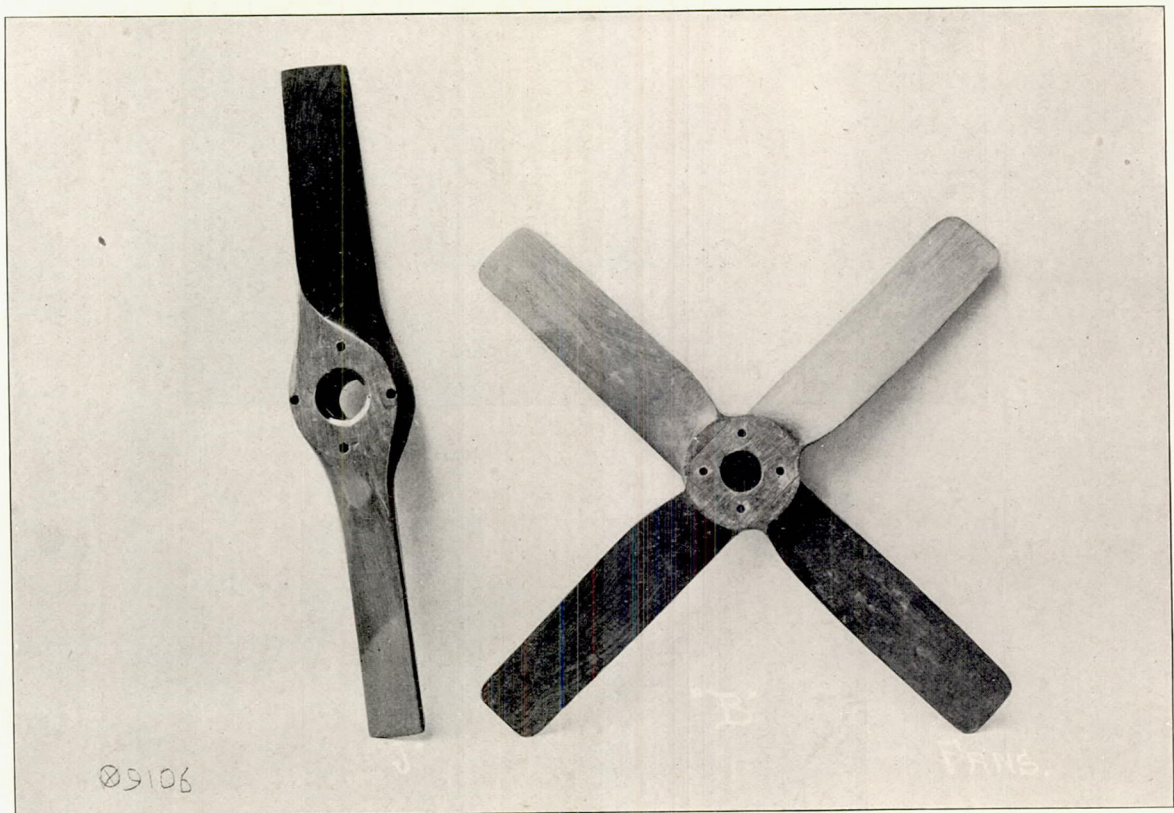


FIG. 5.

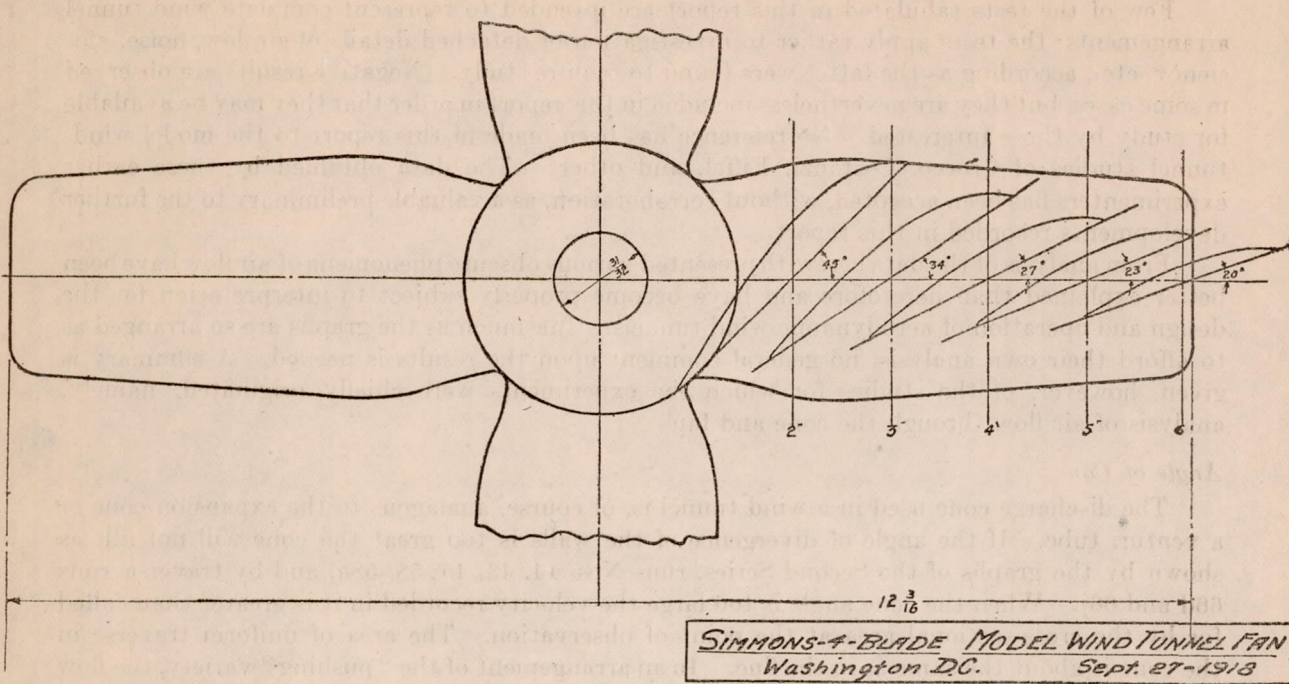


FIG. 3.

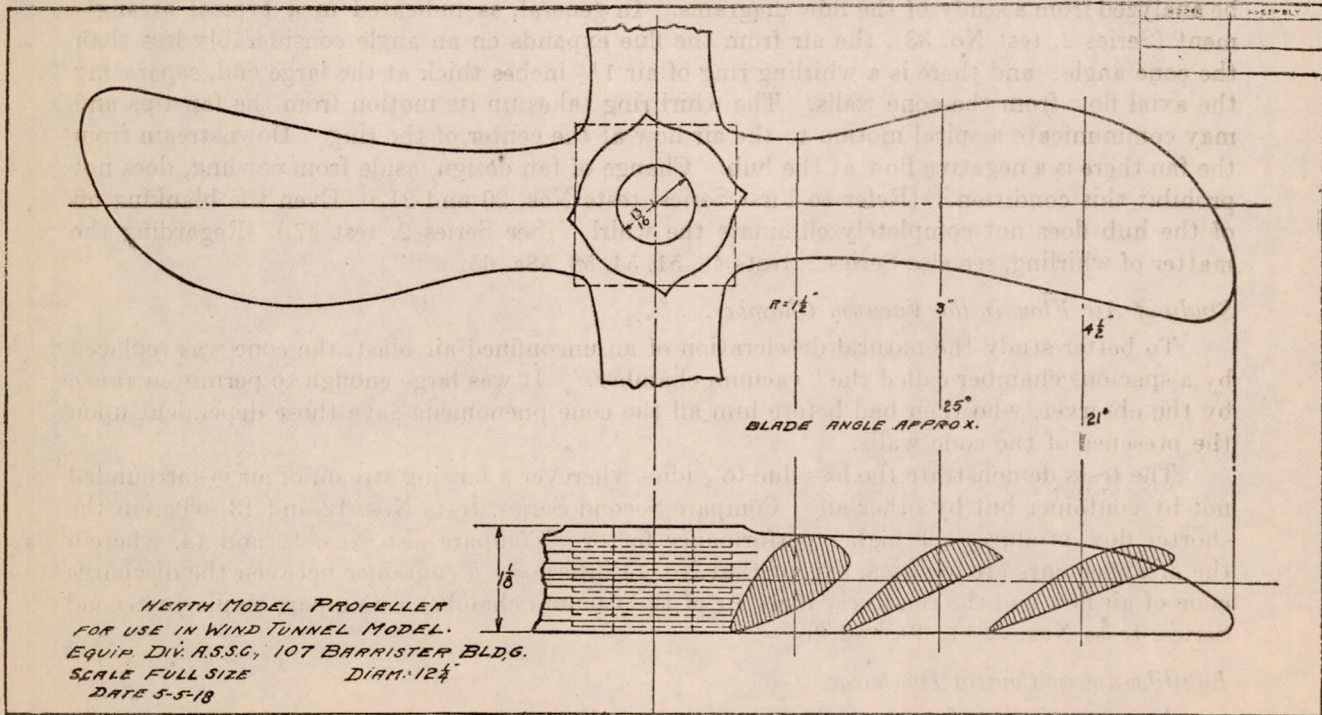


FIG. 4.

DISCUSSION OF RESULTS.

Few of the tests tabulated in this report are intended to represent complete wind-tunnel arrangements; the tests apply rather to investigation of detached details of air flow, noise, efficiency, etc., according as the latter were found to require study. Negative results are observed in some cases, but they are nevertheless included in this report in order that they may be available for study by those interested. No reference has been made in this report to the model wind-tunnel studies of Crocco, Costanzi, Eiffel, and others. The data obtained by these earlier experimenters has been accepted, without corroboration, as a valuable preliminary to the further developments recorded in this report.

From analysis of the data herewith presented various obscure phenomena of air flow have been better explained than heretofore and have become properly subject to interpretation for the design and operation of aerodynamic wind tunnels. Inasmuch as the graphs are so arranged as to afford their own analysis, no general comment upon the results is needed. A summary is given, however, of the studies for which the experiments were chiefly originated, namely, analysis of air flow through the cone and fan.

Angle of Cone.

The discharge cone used in a wind tunnel is, of course, analagous to the expansion cone of a venturi tube. If the angle of divergence of the walls is too great the cone will not fill, as shown by the graphs of the Second Series, runs Nos. 14, 43, 45, 58, 58a, and by traverse runs 66d and 66j. When the cone angle is too large the velocity recorded in it is greater than called for by the cross-sectional area at the point of observation. The area of uniform traverse in the cone is about the same as in the flue. In an arrangement of the "pushing" variety, the flow in the cone tends to hug the walls better, due to the centrifugal whirling of the air. (Refer to the Second Series, tests Nos. 52, 53, and 54.)

Whirls in the Wind Tunnel.

The whirling noticed in the wide-angle cone of the conventional type of wind tunnel may be analyzed from a study of the flow diagrams. In general, as indicated in a typical arrangement (Series 2, test No. 33), the air from the flue expands on an angle considerably less than the cone angle; and there is a whirling ring of air $1\frac{1}{2}$ inches thick at the large end, separating the axial flow from the cone walls. The whirl ring takes up its motion from the fan tips and may communicate a spiral motion to the air flow at the center of the ring. Downstream from the fan there is a negative flow at the hub. Change of fan design, aside from cowling, does not prohibit this condition. (Refer to First Series, tests Nos. 20 and 21.) Even the blanking off of the hub does not completely eliminate the whirl. (See Series 2, test 47.) Regarding the matter of whirling, see also Series 2, tests 48, 51, 54, 58, 58a, 65.

Study of Air Flow in the Vacuum Chamber.

To better study the natural deceleration of an unconfined air blast, the cone was replaced by a spacious chamber called the "vacuum chamber." It was large enough to permit entrance by the observer, who then had before him all the cone phenomena save those dependent upon the presence of the cone walls.

The tests demonstrate the loss due to eddies wherever a flowing stream of air is surrounded not by container but by other air. Compare Second Series, tests Nos. 12 and 13, wherein the shorter flow produces the higher performance factor. Compare also Nos. 12 and 14, wherein the arrangements are identical except that No. 14 interposes a container between the discharge cone of air flow and the relatively inert air of the vacuum chamber. Compare similarly Second Series, tests Nos. 3, 11, 30, and 36.

Equilibrium in Conical Discharge.

It is seen from reference to First Series, tests Nos. 7 and 9, that the air blast leaving the wind tunnel with the cone temporarily in place can be maintained even after the cone is removed; although this conical air blast can not be brought into existence without the use of such a dis-

charge cone. (See also First Series, runs Nos. 22, 23, and 24.) The natural establishment of a virtual cone of air flow is shown in Series 2, test No. 59b, where the fan can be moved 5 inches away from the discharge opening and yet maintain fair flow of air. The existence of the virtual cone is shown by comparing the Second Series, tests Nos. 11 and 20; in No. 11 the air has not expanded sufficiently for the diameter of the fan, with the result that it is discharged with a higher radial than axial component. (See also No. 13, where the effect is exaggerated.)

The Fan.

A comparison of different fan housings shows the fan to be properly located when its plane of rotation is upstream from the large end of the cone, as in Series 2, test No. 31. (Compare Nos. 31 to 34, also 43, 45, 46.) Should a cylindrical housing be used, as in the National Physical Laboratory type, refer to test 55 for indication of the best position for the fan. A cone terminating in a restricted discharge opening is not superior to one terminating in a cylinder. (Compare Series 1, tests 56 and 57.)

Tip clearance was studied in Series 2, test 45, by moving the fan axially to successive positions. It is seen that an increase of clearance from $\frac{1}{48}$ of the radius to $\frac{4}{48}$ of the radius drops the performance factor 12 per cent. In the particular arrangement shown, the clearance should be a minimum; however, it does not follow that generous clearances are always detrimental, for certain other arrangements give very good results with comparatively large clearance

Tests 47 to 51, Second Series, deal with the matter of cores or cowling applied to the fan.

Various investigations were made of the discharge blast from the fan. The parasite whirl occurs as a ring separating the positive and negative air flow; or it occurs some times outside the positive air flow. (See Series 2, tests 31, 70, 43, and 59-a). The effect of confining the fan blast in a Venturi discharge is shown for various arrangements in Series 2, tests 28, 29, 30, 36, 36-a, 37-a, 37-b, 60, 61, 62. Further investigation of confined flow of the fan blast is made by setting up the fan as a "pusher" at the wind-tunnel intake. There results, of course, a helical flow in the flue which is excessive, as would be expected, only when flow through the fan is inefficient. (See Series 1, tests 2, 3, 4, 38, 39.) The characteristics of the pushing arrangement are shown in Series 1, tests 1 to 5, and Series 2, tests 52 to 54, and traverses 66-d and 66-e.

One of the important objects of these experiments was to investigate the question of noise made by the fan. (See Series 1, tests Nos. 9, 57, 59, 60, and Series 2, tests Nos. 55 and 59-b.)

RELATION BETWEEN VELOCITY AND EFFICIENCY.

Reference to run 71 indicates a practically constant efficiency from 0 to 85 ft./sec. Beyond 85 ft./sec. the efficiency decreases, instead of increasing, as would be expected.

EFFECT OF INTAKE BELL ON VELOCITY TRAVERSE OF VALUE.

Without an intake bell a "vena contracta" forms at the flue entrance, resulting in loss of energy due to eddy formation, and inferior velocity distribution in the flue. (See run 73.) The inflowing air can, in the early stages of its acceleration, follow a curve of sharp radius, and flows in with radial component as well as axially toward the intake. The inflow is analogous to the inflow to a static propeller; by means of experiment the proper shape of intake bell may be determined as well as the minimum clearance between intake and end wall of the building in which the wind tunnel is housed. The minimum practicable diameter may also be thus determined.

Runs 72 to 76 establish the comparative merits of various intakes, through a study of the velocity traverse in the flue afforded by each type. These tests measure the drop in energy between the room and the point of observation; they give an adequate indication of the velocity traverse, since the static head traverse is substantially uniform. (Run 77.)

Of the types tested the order of preference appears in sequence as follows (see Tests 72-76):

1. Grimes intake.
 2. N.P.L. 7-foot intake
 3. N.P.L. 4-foot intake
 4. No intake.
- } Practically the same.

Velocity Traverse Studies:

In these tests (72 to 76) it is apparent that the velocity traverse is better close to the intake than at a distance. For the Grimes' type intake uniformity exists over 0.93 diameter near the intake, as against 0.77 diameter 20 inches downstream. Run 77 shows that the flow near the entrance is substantially axial at all points of the traverse.

Two conclusions are obvious:

1. The model to be tested should be located as close to the intake as is permitted by local distortions in the airflow lines about the model.

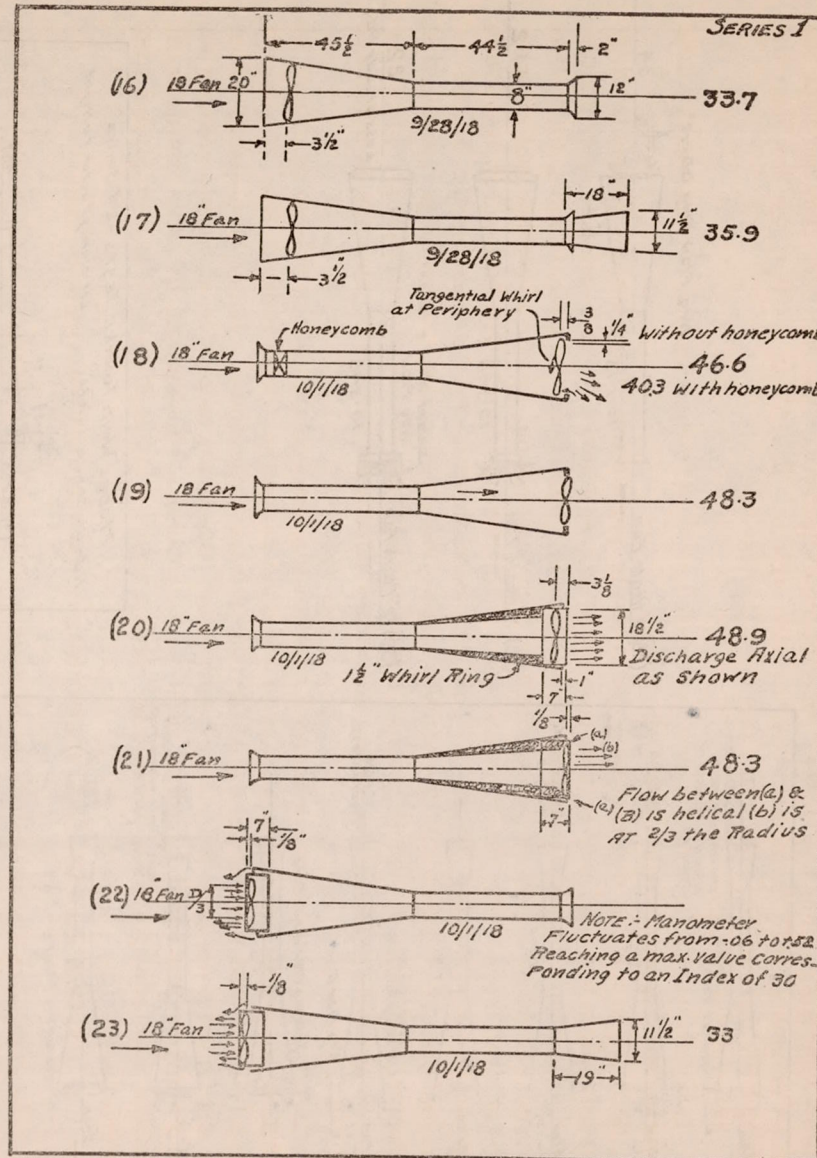
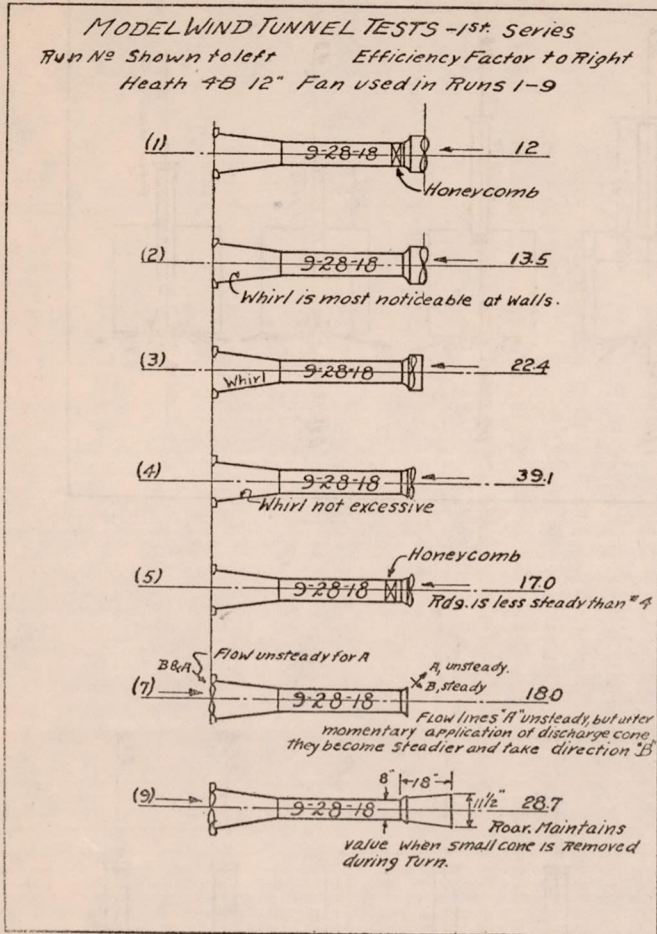
2. A honeycomb is not necessary for securing parallelism of the airflow filaments where proper intake is installed, and is to be considered only as a device for decreasing velocity fluctuations in the flue. Regarding velocity fluctuations or "pulsations" in a wind tunnel, the writers have not succeeded in solving the problem to their satisfaction. After taking account of variations in mean flue velocity due to inconstancy of the pressure causing the flow, it has been found that serious "pulsations" remain. This has been investigated by reading the differential dynamic pressure between any two points in the flue cross section; the readings indicate that in general pulsations at the two points are not simultaneous, but are of local extent. The pulsations are greatest near the flue walls, where they depend on the vortex phenomena associated with skin friction.

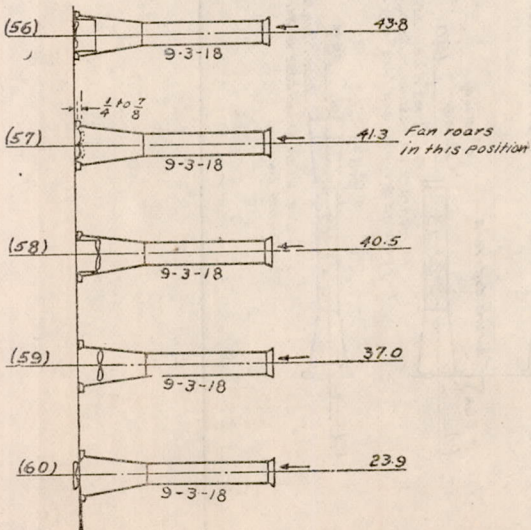
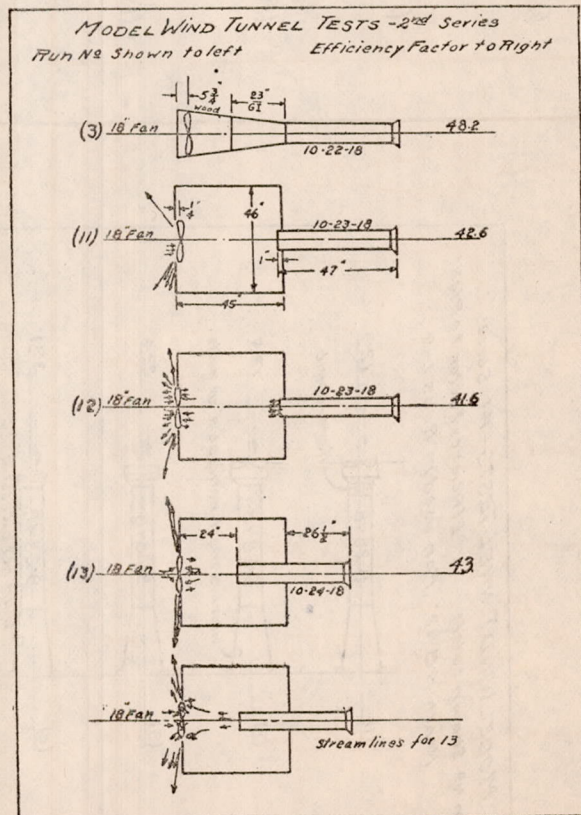
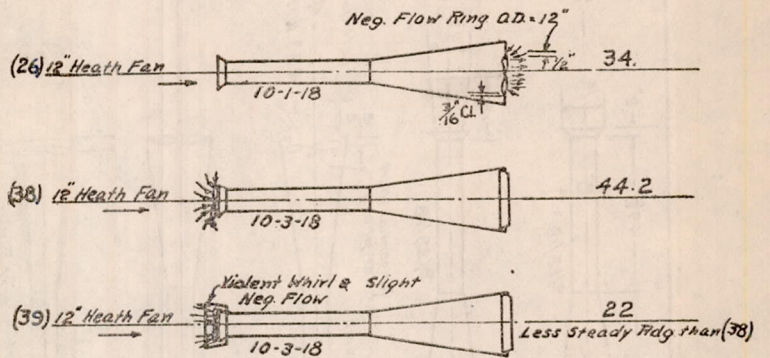
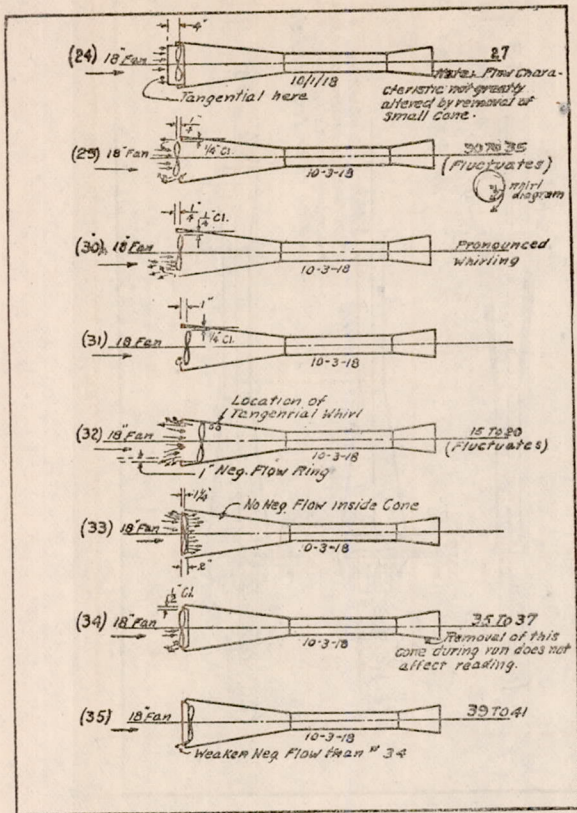
In further discussion of the relation between the honeycomb and the pulsations, it may be said that the pulsations in the McCook Field wind tunnel have been reduced from 15 per cent down to 3 per cent without the use of the conventional honeycomb. It has been assumed that the stream has a tendency to take up a spiral whirl, due to the radial flow at intake. Such whirl can be largely prevented by plane axial vanes located a considerable distance downstream. Hence the installation of the four-blade "straightener" 4 feet long and 4 feet downstream from the model.

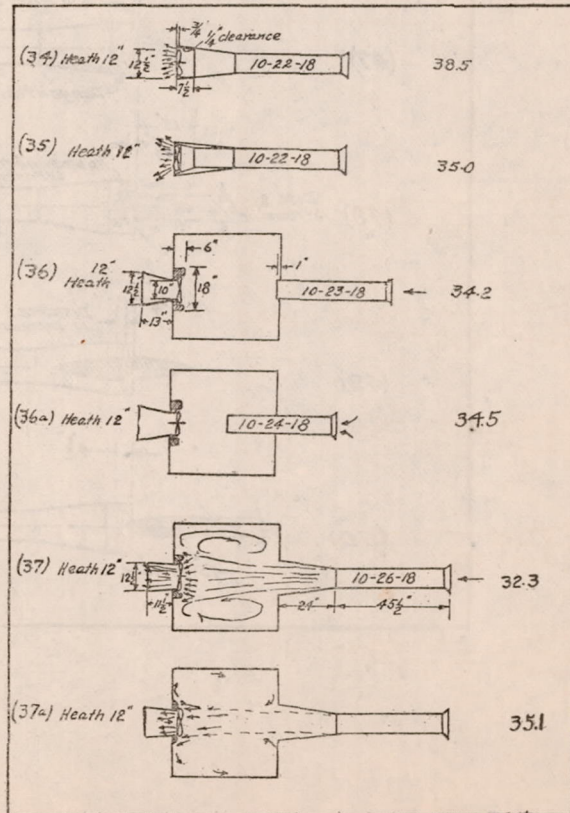
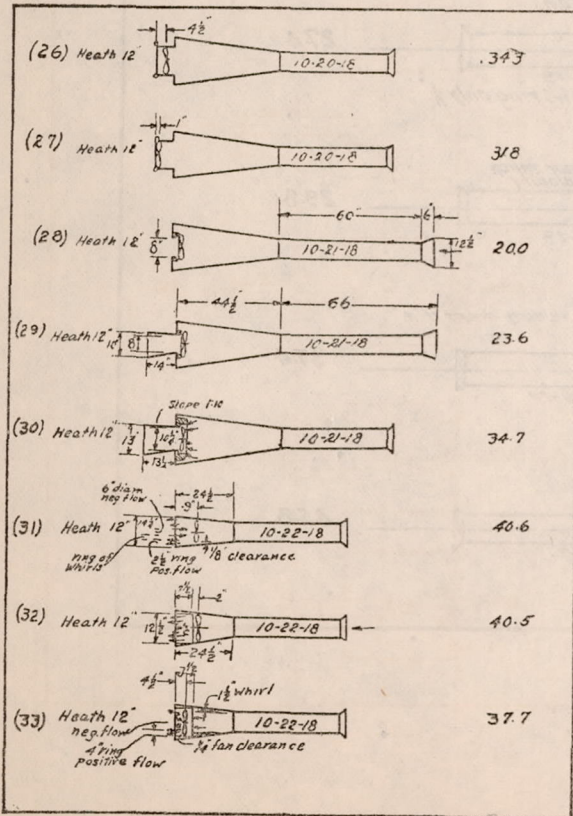
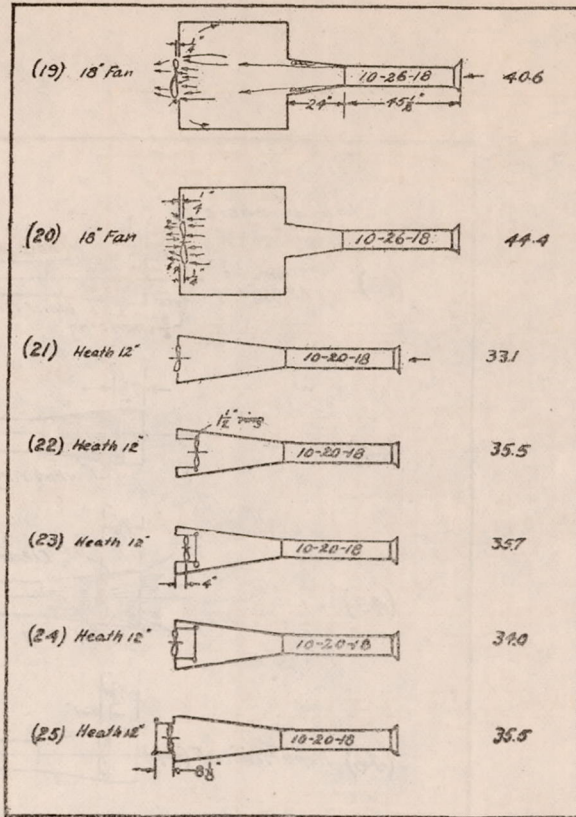
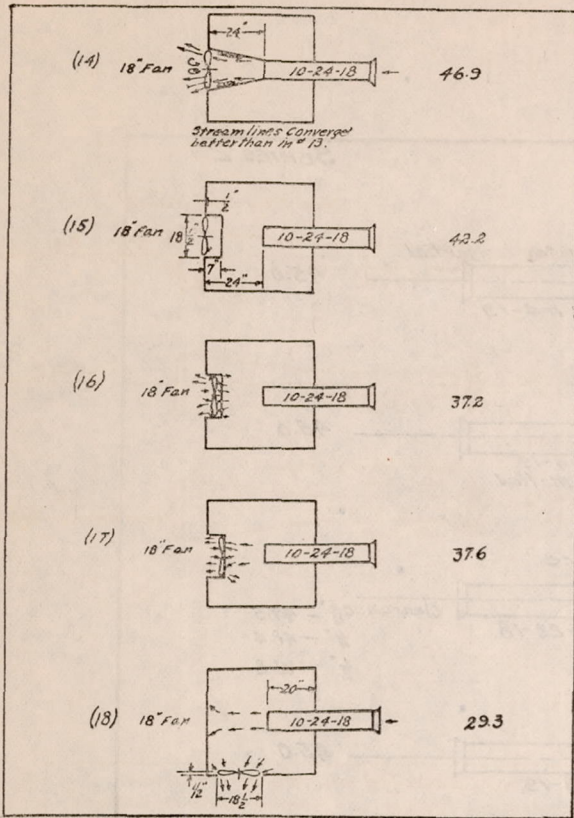
EFFECT OF FAN-CONE ARRANGEMENT ON VELOCITY TRAVERSE IN FLUE.

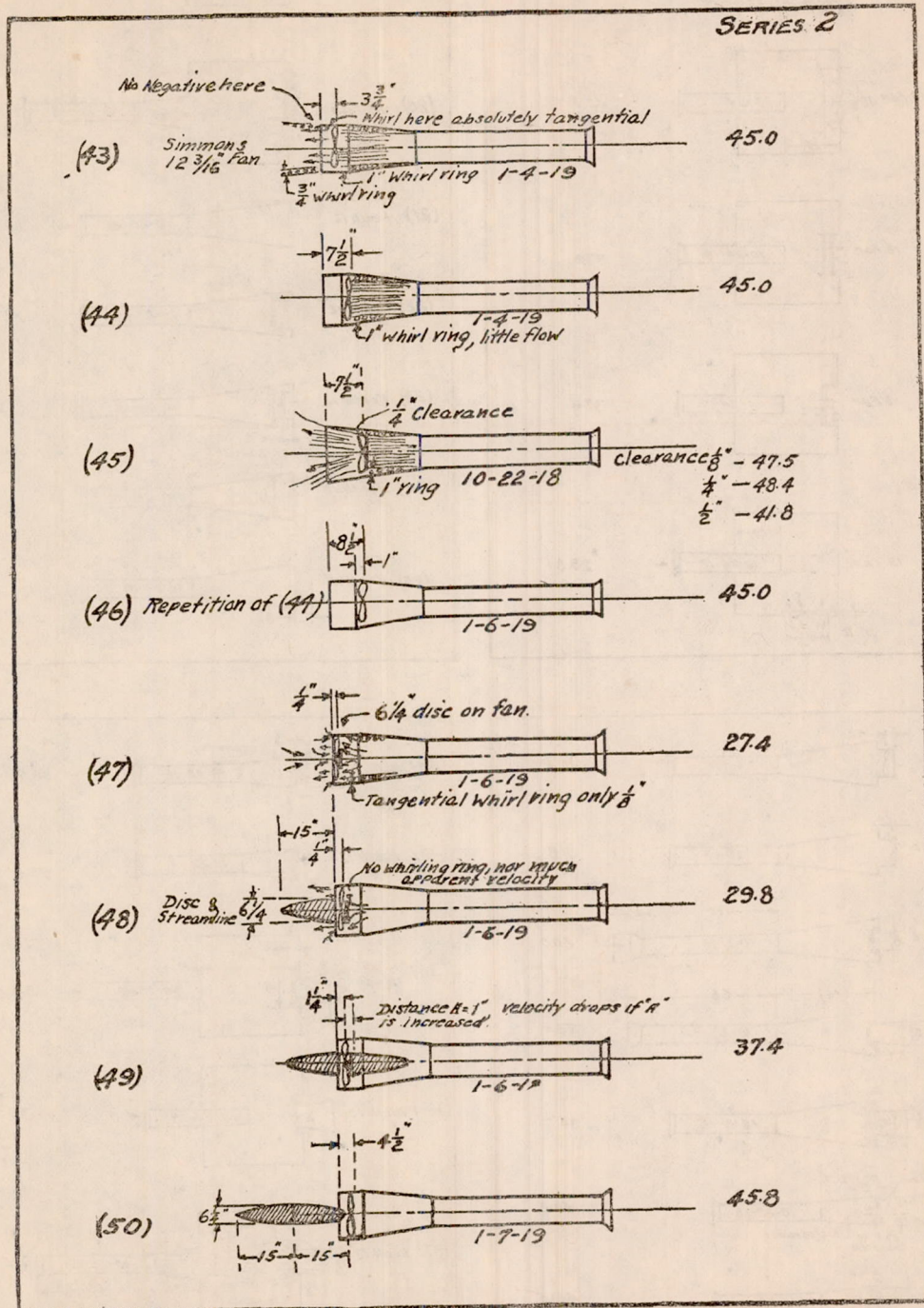
The velocity traverses afford valuable data on the relative merits of the fan-cone arrangement. Refer to Series 2 tests 72, 66-c, 66-f, 66-g, which are made with the same intake bell and flue and without honeycomb. Of these four tests the last three are made with fan propulsion; test 72 is made with a special arrangement, the cone being removed, and the flue being sealed into the intake of the 14-inch McCook Field wind tunnel so that its flow is in effect created by a uniform "suction" rather than by a propeller.

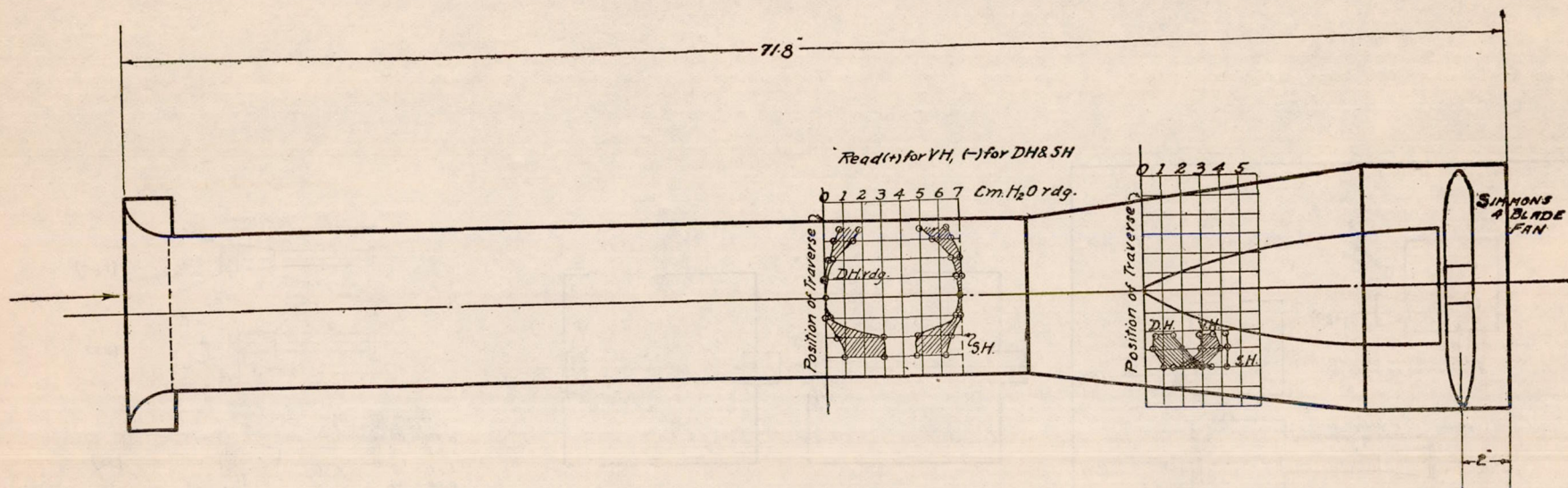
Comparison of these tests shows that the traverse uniformity varies with the fan-cone arrangement; it is best when the suction is uniform and inferior when the suction is less uniform. Of course the static head traverse at the fan is not uniform, and from tests 66-c, 66-f, and 66-g it appears that this nonuniformity of static head traverse affects the portion of the flue occupied by the model.



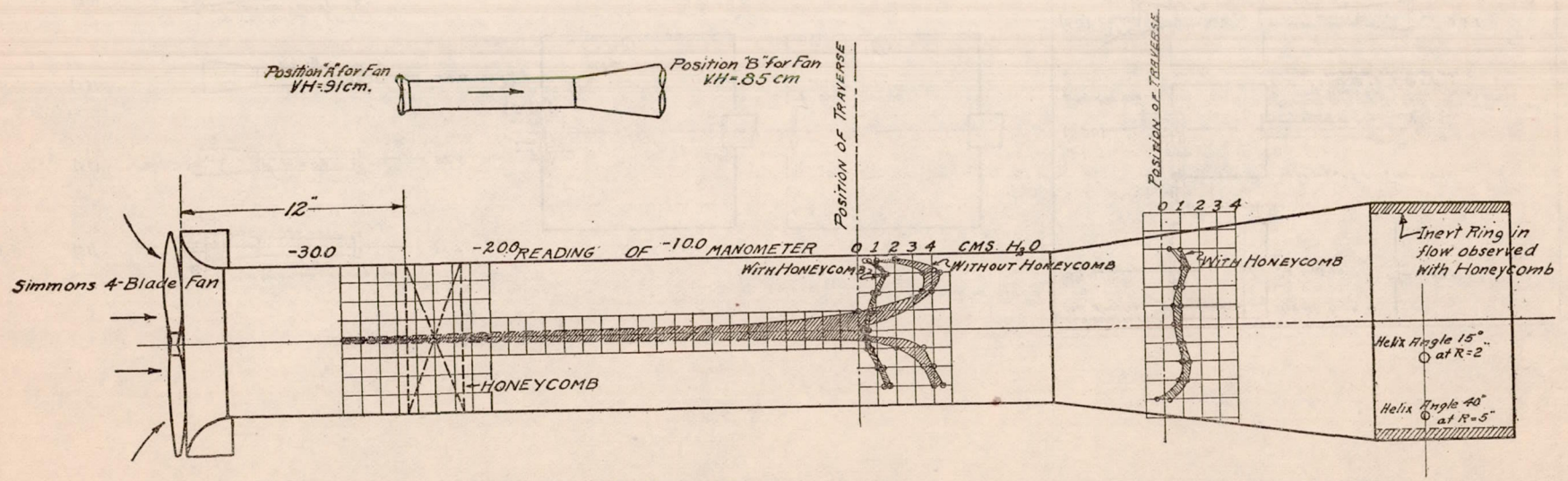




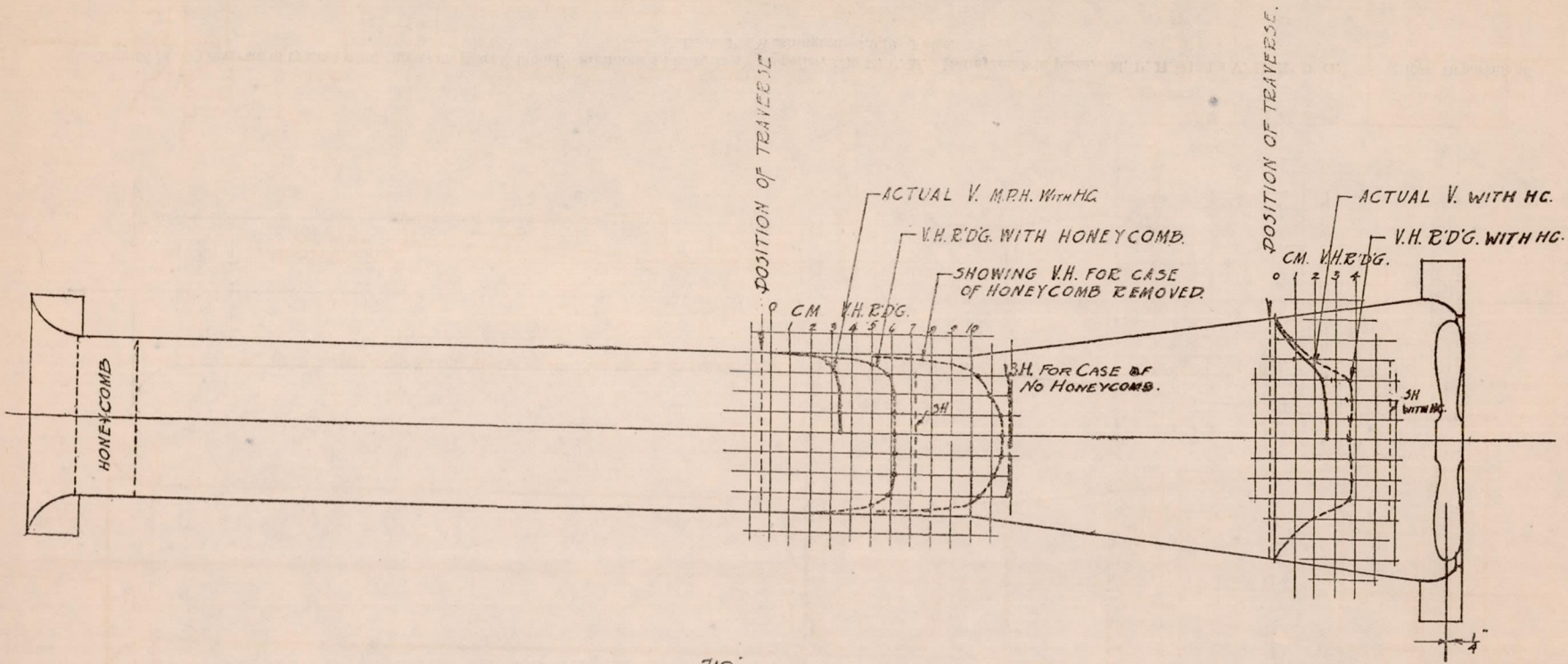




Traverse of air flow. Model wind tunnel having core in cone. Test No. 66 (c) 1-8-19. Fan 2" inside discharge place. No honeycomb; discharge sleeve in place. Washington, D. C.

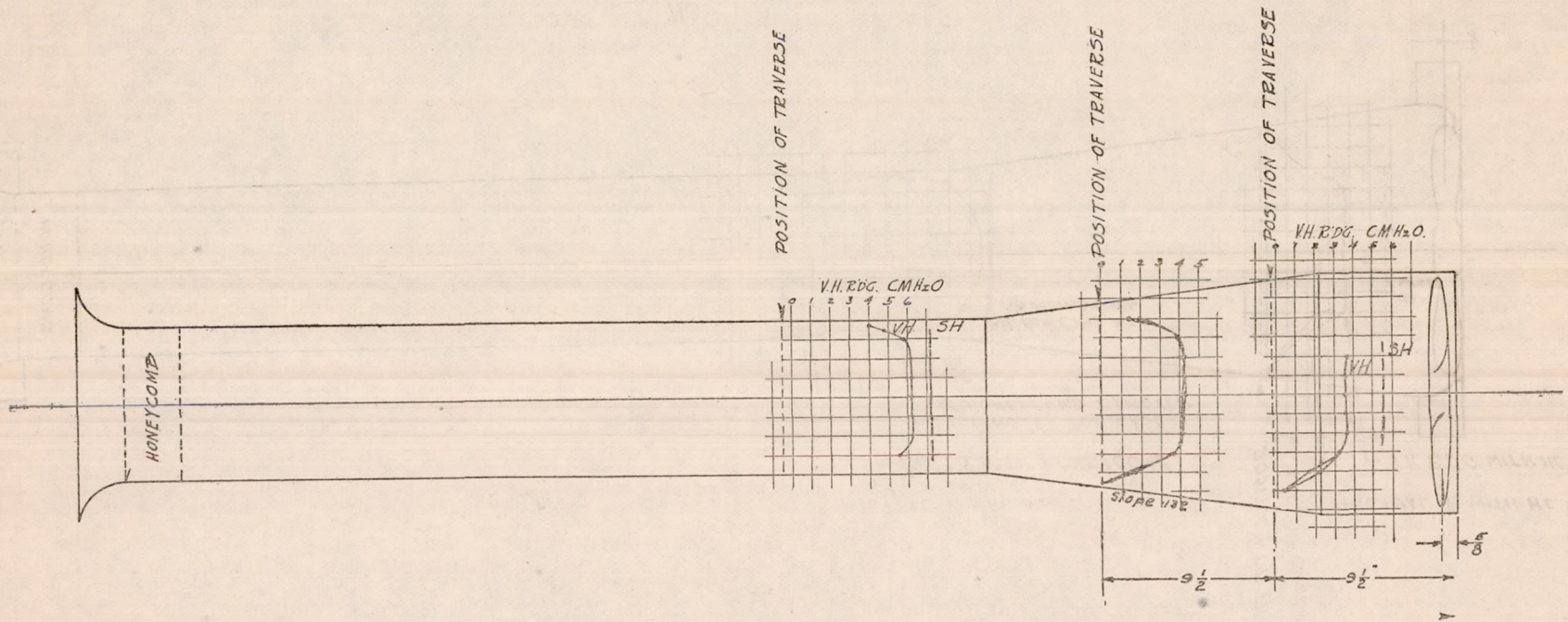


Dynamic heads. Model wind tunnel test Nos. 66 (d) and 66 (e). Fan at intake 2590 R. P. M. Sleeve and honeycomb in place. Washington, D. C. Date, Jan. 9, 1919.

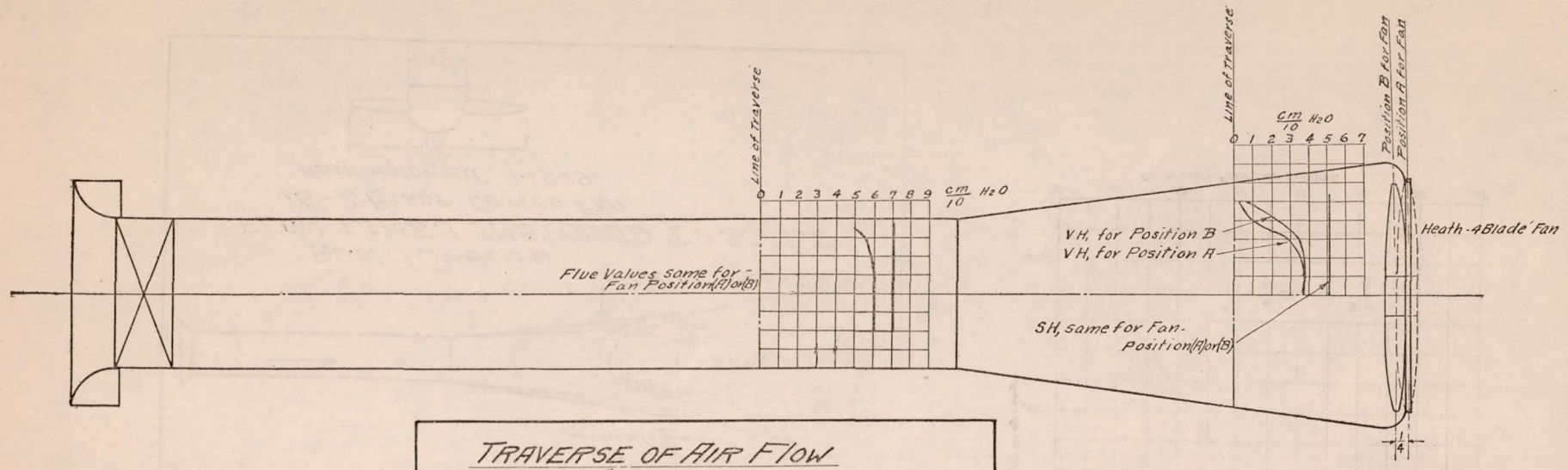


718

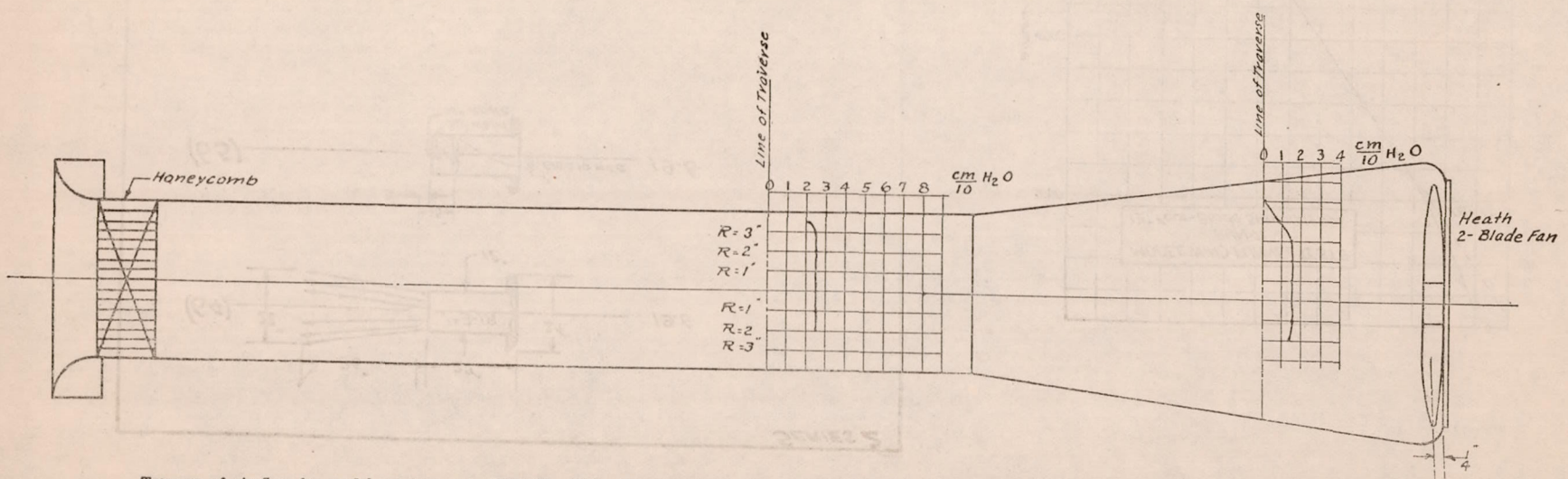
n 66 (f). Traverses of typical wind tunnel on $\frac{1}{2}$ scale model. Heath 4-blade, 12" propeller, 2500 R. P. M. Comparison of traverse with and without honeycomb. Sci. and Res. Department. B. A. P. Washington-1:19:19-Fales.



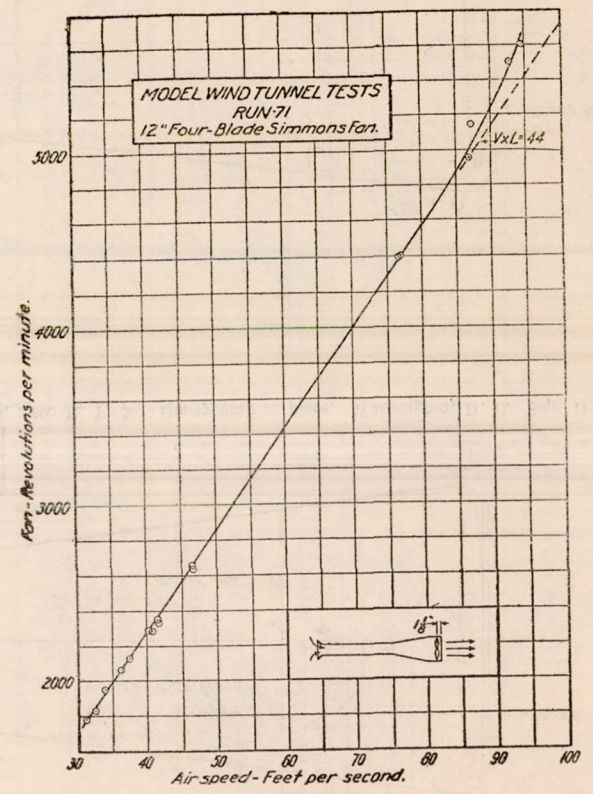
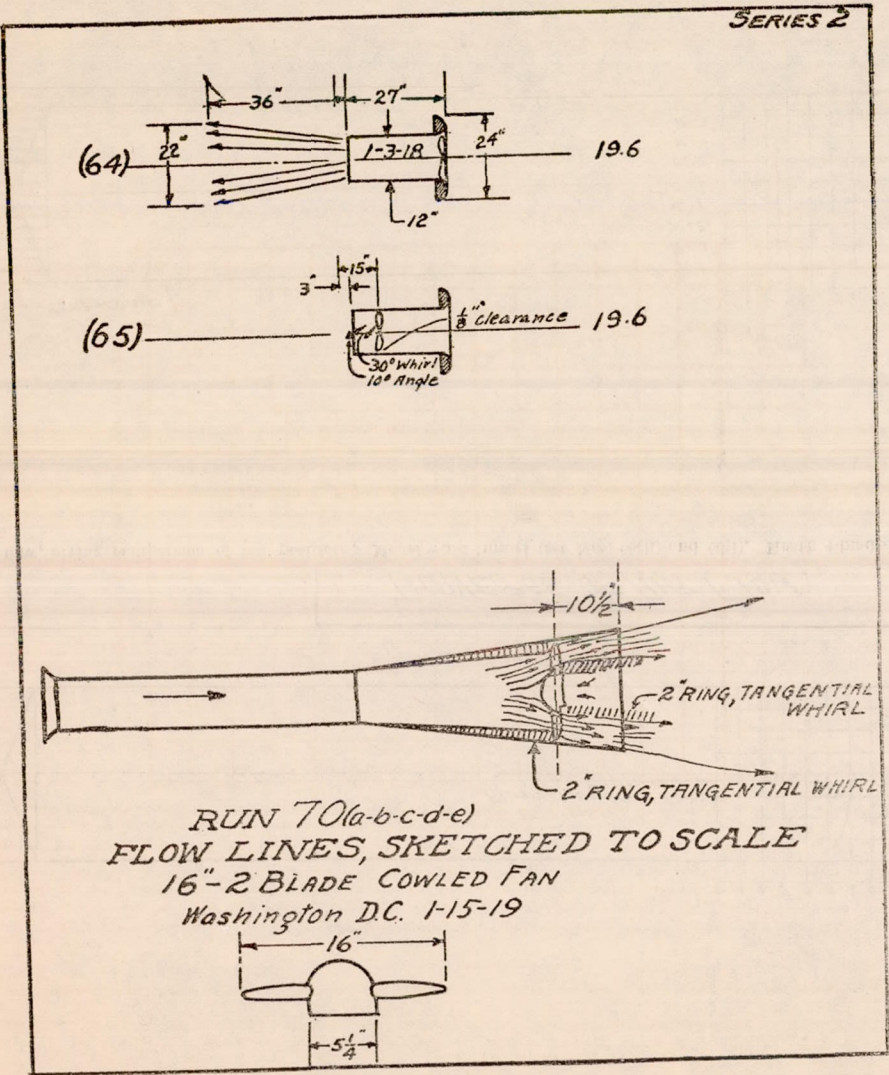
Run 66 (g). Traverses of typical wind tunnel on $\frac{1}{2}$ scale model. Simmons 4-blade, $12\frac{1}{8}$ " propeller, 2240 R. P. M. Honeycomb in place. M. P. H.=13.1 x V. H. R' D' G. Sci. & Res. Department. B. A. P. Washington-1:9:19-Fales.

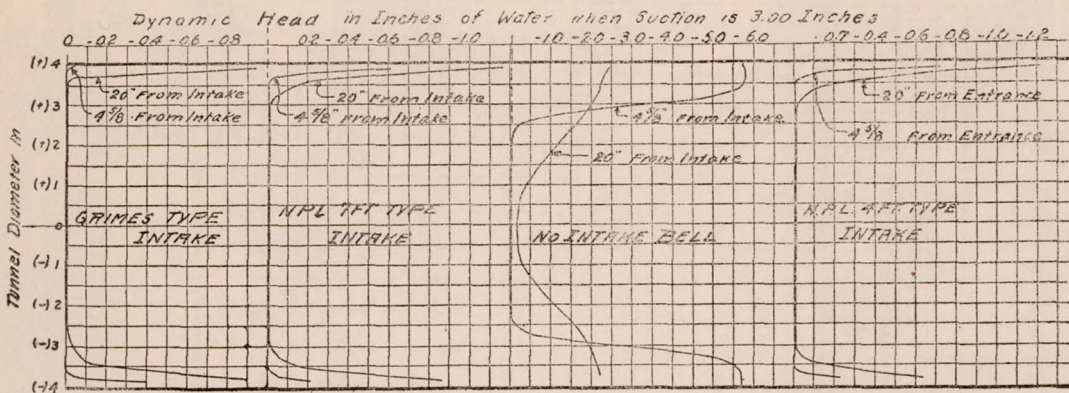


Traverse of air flow, giving comparison of fan positions. Model wind tunnel test Nos. 66(h) and 66(i). Heath 4-bladed 12-inch fan, 2,500 R. P. M. Honeycomb in place. Washington, D. C. Sept. 11, 1918.

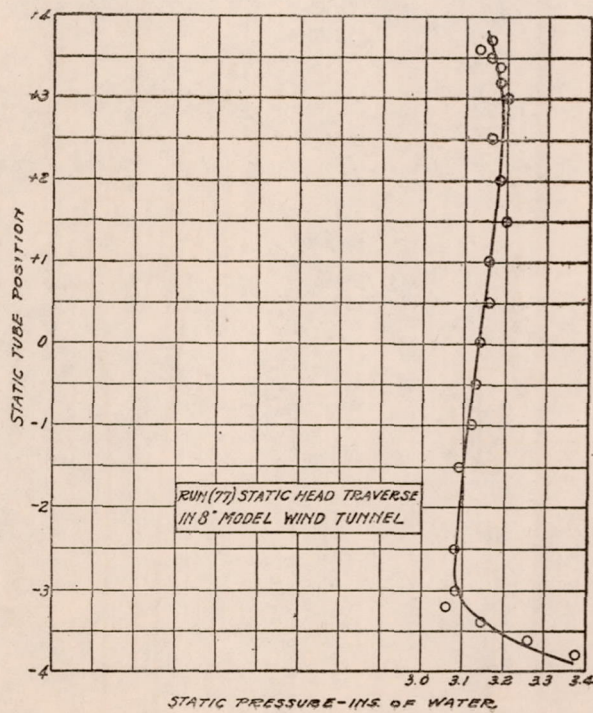


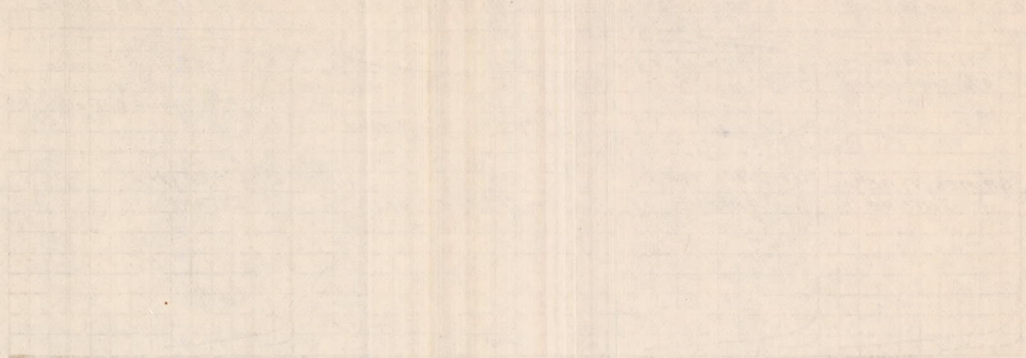
Traverse of air flow for model wind tunnel. Test No. 66(j). Honeycomb in place. Heath 2-bladed 12-inch fan, 2,500 R. P. M. Washington, D. C. Date, Aug. 20, 1918.





DYNAMIC HEADS IN MODEL WIND TUNNEL FLUE
FOR COMPARING VELOCITY TRAVERSES OF DIFFERENT INTAKES
 225 SERIES TESTS 72 TO 76 No Honeycomb used
 Flue connected to Large Wind Tunnel No Cone used
 10-2-19 DAYTON OHIO



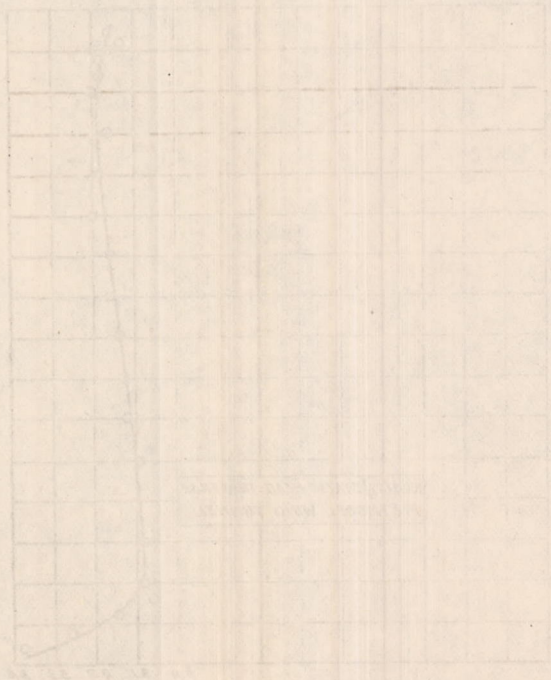


WALL THICKNESS AND TEMPERATURE VARIATIONS AT HIGH PRESSURE

WALL THICKNESS (mm) vs. TEMPERATURE (°C)

Pressure: 10,000 atm

Time: 10 min



WALL THICKNESS (mm) vs. TEMPERATURE (°C)

Pressure: 10,000 atm

Time: 10 min

REPORT NO. 83.

PART II.

THE McCOOK FIELD WIND TUNNEL.

BY F. W. CALDWELL AND E. N. FALES.

The information available on propeller aerofoils in the past has been comparatively meager, and most of it has been obtained at air speeds of about 30 to 60 miles per hour. It has always been a matter of a good deal of concern among aeronautical engineers as to whether the information obtained at these low speeds is reliable when applied to propellers whose velocities are many times greater.

As a matter of interest, tip speeds of some of the propellers in actual use are given below:

	Miles per hour.
USD-9 airplane with Liberty-12 engine.....	650
VE-7 airplane with Hispano-Suiza 150-horsepower engine.....	545
Thomas-Morse airplane with 80-horsepower LeRhone engine.....	380
Verville Chasse airplane with 300-horsepower Hispano-Suiza engine.....	600
Roché XB-1-A airplane with 300-horsepower Hispano-Suiza engine.....	625
Curtiss JN-4 airplane with Curtiss OX-5 engine.....	420
DH-9 airplane with Rolls-Royce 375-horsepower engine.....	430

It is evident that the speeds given above are so far in excess of the usual wind-tunnel speed as to justify a little skepticism in applying results obtained in the slow-speed tunnel.

The results of many static tests of propellers have shown that the horsepower does not vary directly as the cube of the revolutions per minute, but increases much more rapidly than the cube at very high tip speeds. It has consistently been shown, as the result of a large series of static tests carried out by the writers, that the ratio of thrust to torque varies considerably with revolutions per minute. At the same time wind-tunnel tests on propellers have indicated that the experimental no-thrust pitch increases somewhat with the revolutions per minute of the propeller.

These considerations have resulted in the inauguration of a series of wind-tunnel tests at very high speeds in order to investigate scaling effect on the lift and drag coefficients due to such speeds.

During the winter of 1918 it was proposed by the engineering division at McCook Field to erect a small tunnel, primarily for the calibration of instruments. (See fig. 6.) The writers, working in conjunction with Mr. C. P. Grimes, determined the design of this tunnel for the attainment of the greatest possible speed with the power available, so as to adapt the apparatus to model tests of propeller aerofoils.

DESCRIPTION OF McCOOK FIELD 14-INCH WIND TUNNEL.

As in other wind tunnels, air is sucked through a horizontal tube, where it blows against a small model at known velocity. The model is supported by a rod projecting from a suitable balance into the tunnel, and the forces concerned in flight can thus be measured. The air after passing the model is decelerated in an expanding cone and exhausted into the room by a propeller fan. Description of the McCook Field tunnel need include only those features which differ from the standard type.

The intake trumpet, tube, and expanding cone have the general form of a Venturi tube with a length of $18\frac{2}{3}$ feet; the intake trumpet has a diameter of $3\frac{1}{2}$ feet and radius of curvature of $22\frac{3}{4}$ inches; the throat diameter is 14 inches and the fan diameter is 5 feet. (See fig. 10.) The location of the test section close to the intake is advantageous, as discussed

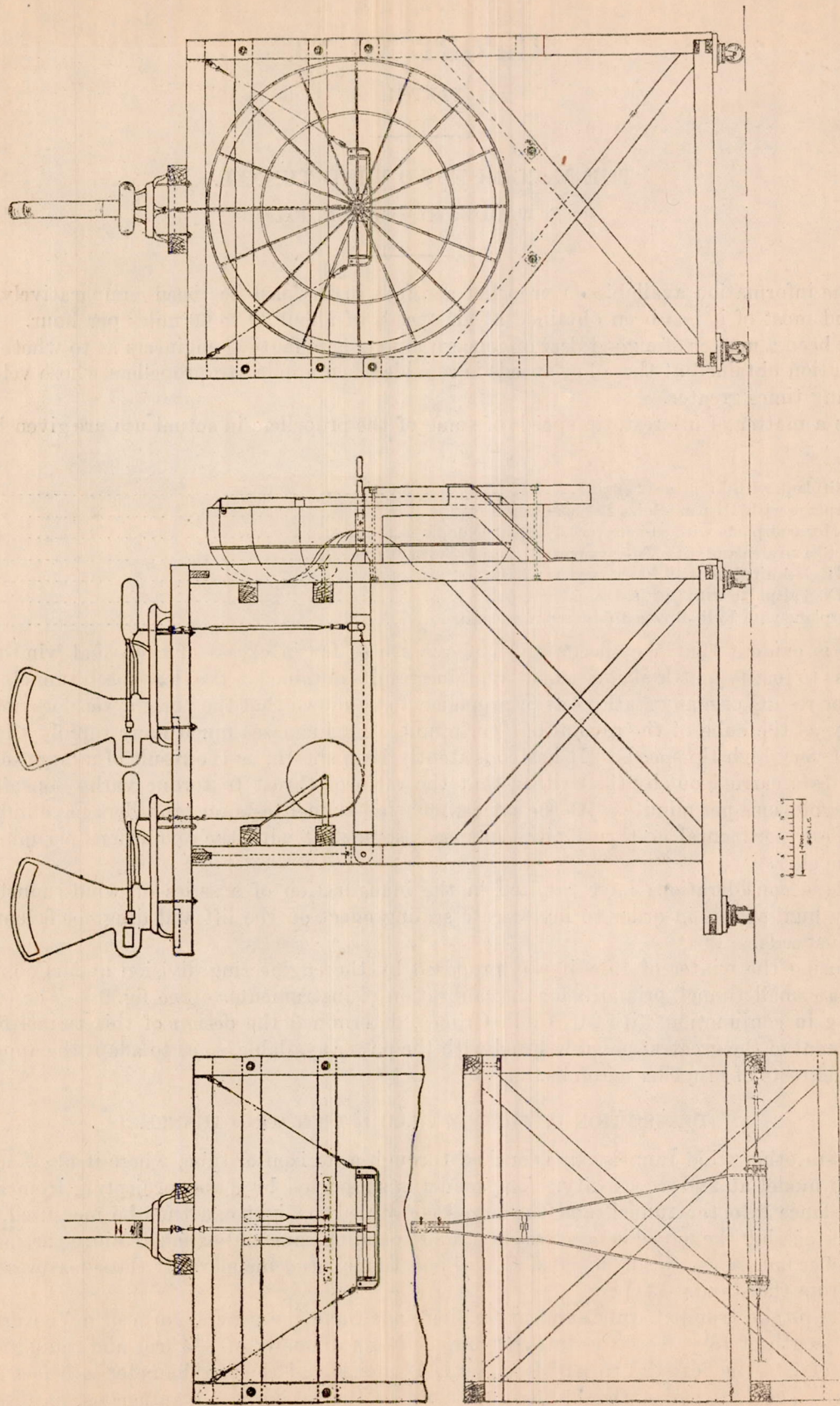


Fig. 9.—Weighing mechanism and entrance vanes for high-speed wind tunnel.

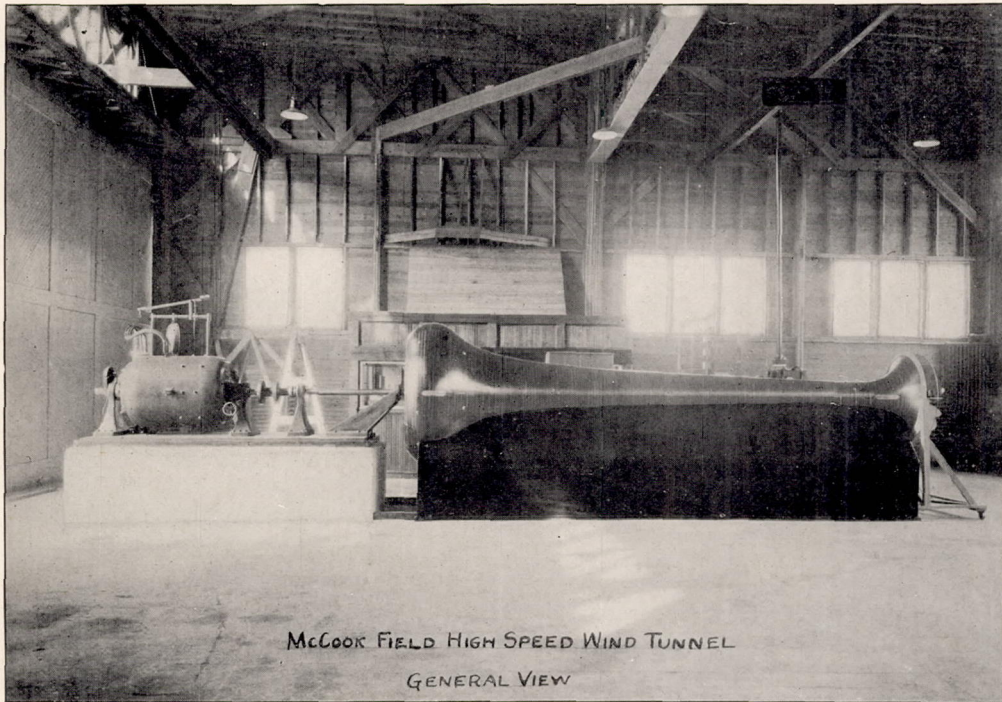


FIG. 6.

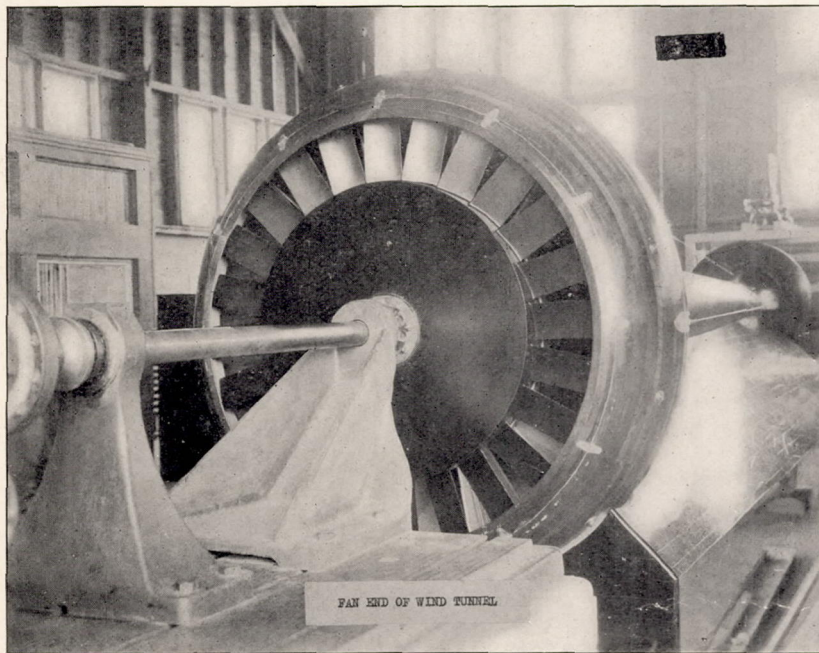
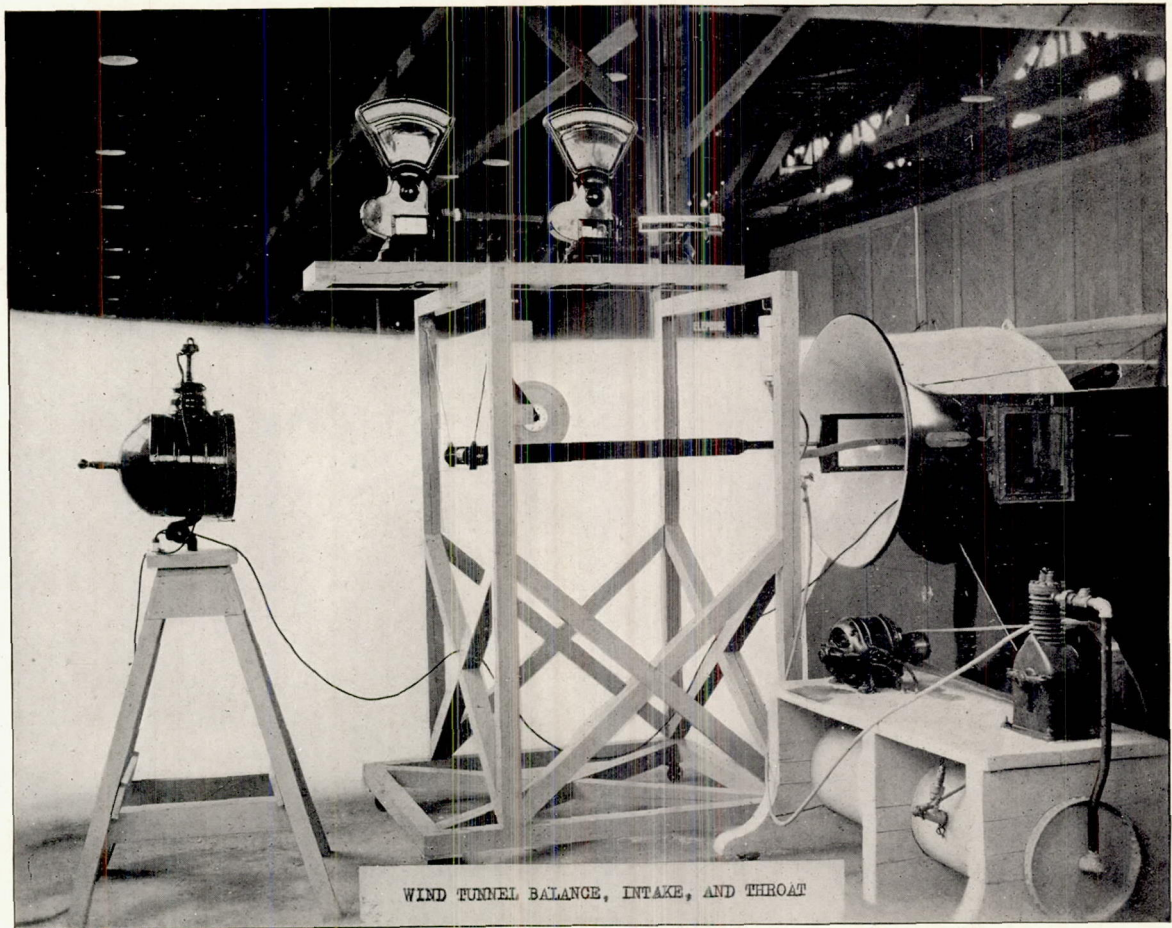


FIG. 7.



WIND FUNNEL BALANCE, INTAKE, AND THROAT

FIG. 8.

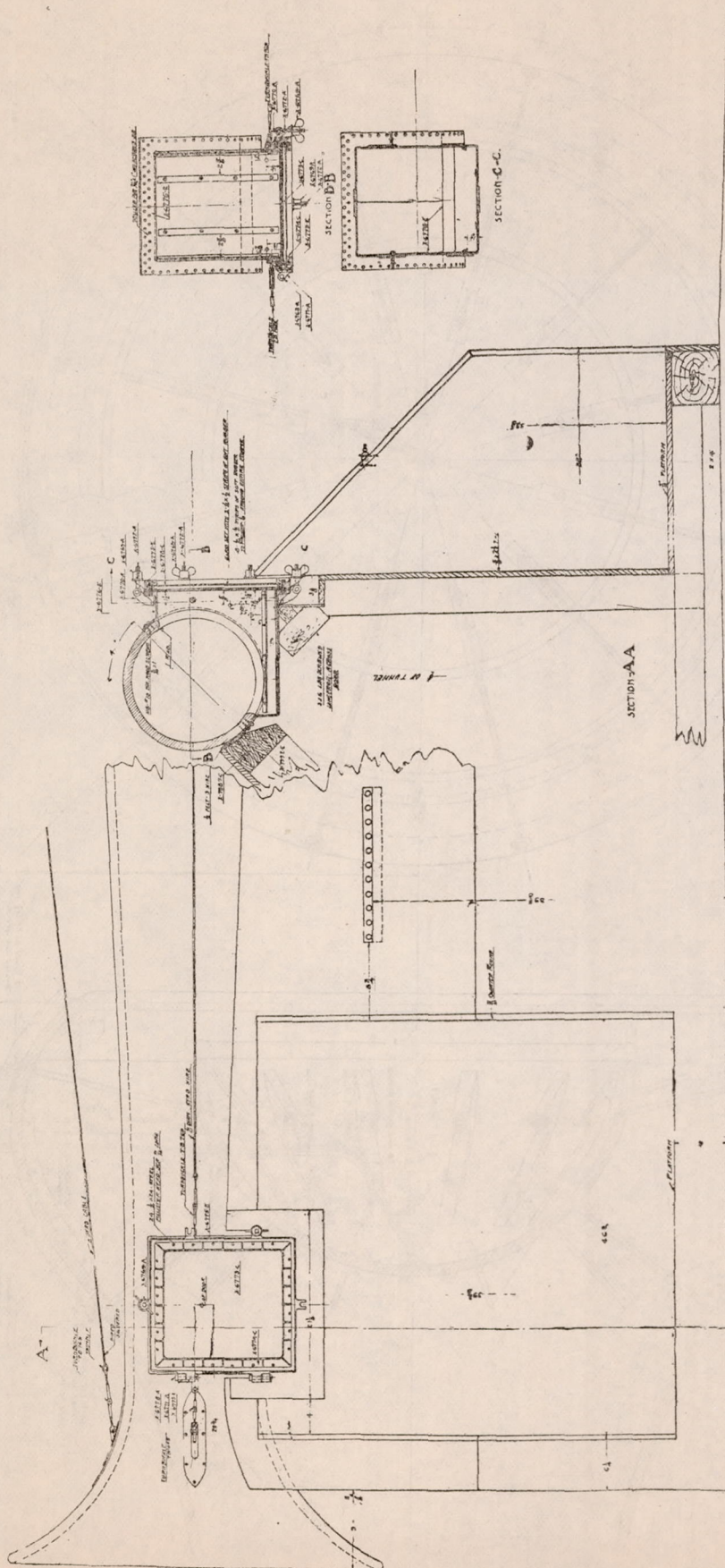


FIG. 10.—Entrance and throat of high-speed wind tunnel.

in section 1 of this report; there is no appreciable loss of energy at the intake, and the traverse of a diameter at the commencement of the throat shows no appreciable velocity variation except at the walls. The usual honeycomb is omitted, but a four-bladed "straightener" 48 inches long is inserted in the cone 4 feet downstream from the model, and there is a straightener outside the intake having 16 flat radial blades. The former "straightener" cuts the fluctuations of the velocity from 15 per cent down to 2 per cent. The cone is of 5° angle for the first 100 inches.

The power plant consists of a Sprague dynamometer, capable of delivering 200 horsepower for one-half hour at 250 volts and 1,770 revolutions per minute without overheating. The 5-foot fan is made with a solid center disk 40 inches in diameter, and has 24 blades 10 inches long. At the upstream side of the 40-inch disk, a bell of equal diameter is fixed in the tunnel so that the air is led up to the annular discharge opening with a minimum of eddies. (See fig. 11.)

The balances are of two types. The first one (fig. 9), designed by C. P. Grimes, measures lift and drift on two separate instantaneous-reading Toledo scales. It is mounted upon a portable carriage. The spindle for the model projects horizontally and axially from this carriage into the mouth of the wind tunnel, carrying the model at its free end. The spindle terminates in a thin, flat bar, the latter clamping a graduated disk which is rigid with the model at the center of the span. This type of balance possesses three advantages, as follows: (1) Instantaneous readings make it possible to synchronize balance and velocity observations and to practically eliminate the effect of velocity fluctuations; (2) the air forces can be qualitatively studied, as, for instance, in the case where a given set-up has two values of K_y , when the balance can be seen to change from one reading to another; (3) the method of support affords a highly accurate means of skin friction observation.

The second type of balance is of the "vector" type, invented by the Wright Bros., with improvements developed by the writers; the principle is indicated in the sketch figure 18. This balance reads L/D with an accuracy superior to the ordinary type; and it reads lift and drift in terms of static pressure. The advantage of the latter feature is that the reading is deadbeat.

OPERATION OF THE WIND TUNNEL.

The method of carrying out the test consists in setting the model in the tunnel at a known angle of attack and measuring the lift and drift forces by means of the indicating Toledo scales. As the precision of these instruments is better than one-tenth per cent, they are considered sufficiently accurate for work of this kind. The three readings of velocity head, lift, and drag are taken by three different observers, the readings being synchronized by means of signals. The tunnel is run at speeds varying for each angle, from about 30 miles per hour to about 450 miles per hour; lift, drag, and velocity-head readings being taken at each speed.

In order to check up the direction of the wind in the tunnel the model is turned upside down and the run repeated with the model set at the same angle. By this means it is found that there is a fairly uniform correction of about 0.4° . This correction has not been applied to the small charts showing K_y for a given angle at various speeds, but has been applied to the larger chart in the center showing K_y plotted against angle.

An observer at the lift scale chooses a point about which the indicator hovers, and when the pointer is so hovering he makes a signal; a second observer on the drift scale, and a third observer at the manometer then make simultaneous observations, each observer having previously become accustomed to the respective lag between his instrument and that of the observer who gives the signal. In this way the fluctuations of velocity in the wind tunnel become less important for accurate results. An automatic recording device for doing the work of the observers at once suggests itself, assuming that the various instruments are properly synchronized. The development of such an instrument has been investigated but not completed.

The tests are made with an increasing velocity; that is, the motor is started at a low r. p. m., a set of readings taken, and then the motor speed increased by means of a rheostat. Occasional

check runs are made with decreasing speeds. Where speeds are approached at which the flow becomes unstable, the condition is easily observed upon the balances, which may be seen to hover successively at two distinct points, the speed remaining the same.

EFFICIENCY OF THE WIND TUNNEL.

The question of efficiency of the wind tunnel is one which was made the subject of much preliminary study. By efficiency is understood the ratio of kinetic energy of the air stream at the throat of the tunnel minus the energy absorbed by the fan, all divided by the energy of the air stream at the throat.

$$e = \frac{\frac{\rho}{2g}AV^3 - E}{\frac{\rho}{2g}AV^3}$$

where $\frac{\rho}{g}$ is the density, A the cross sectional area of the throat, V the velocity at the throat, and E the rate of absorption of energy by the fan.

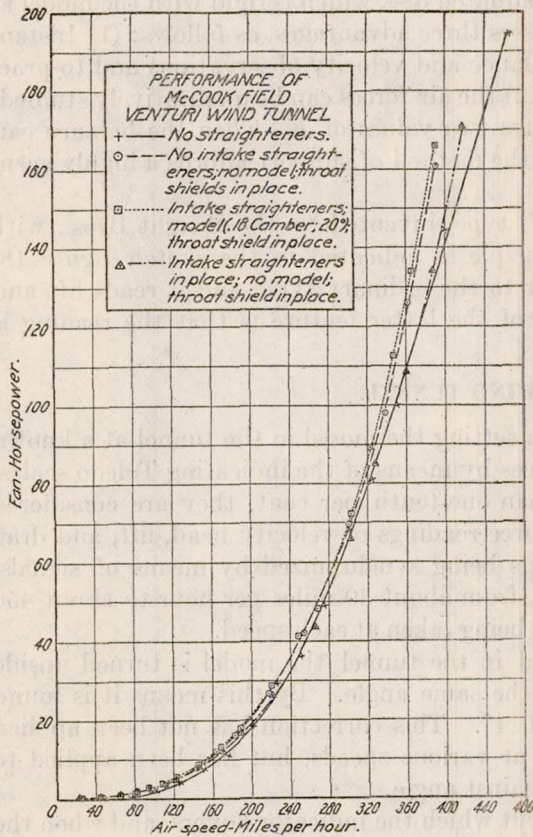


FIG. 14.

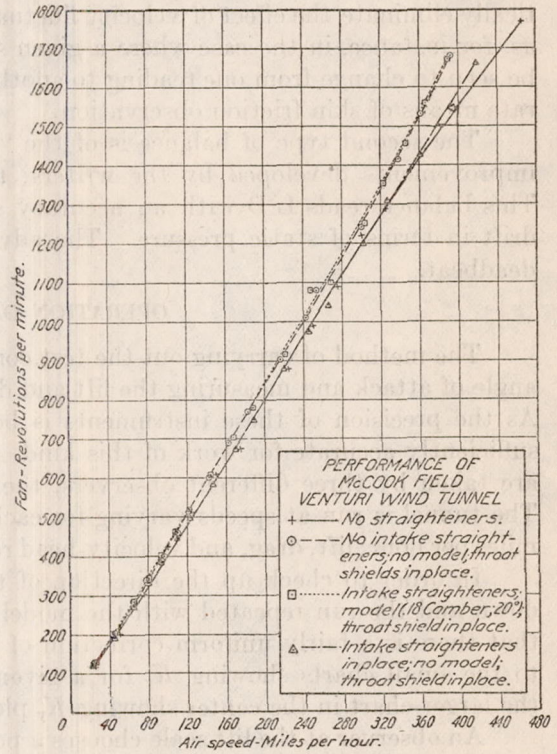


FIG. 15.

It is to be noted that this ratio differs from the conventional efficiency factor used in wind-tunnel discussions (kinetic energy at throat over fan energy). It is treated in note II of this report. A value of 76 per cent was reached, higher than has been usual in determining aerofoil coefficients in other wind tunnels. The five curves of figures 14 and 15 show the performance of the wind tunnel under different conditions.

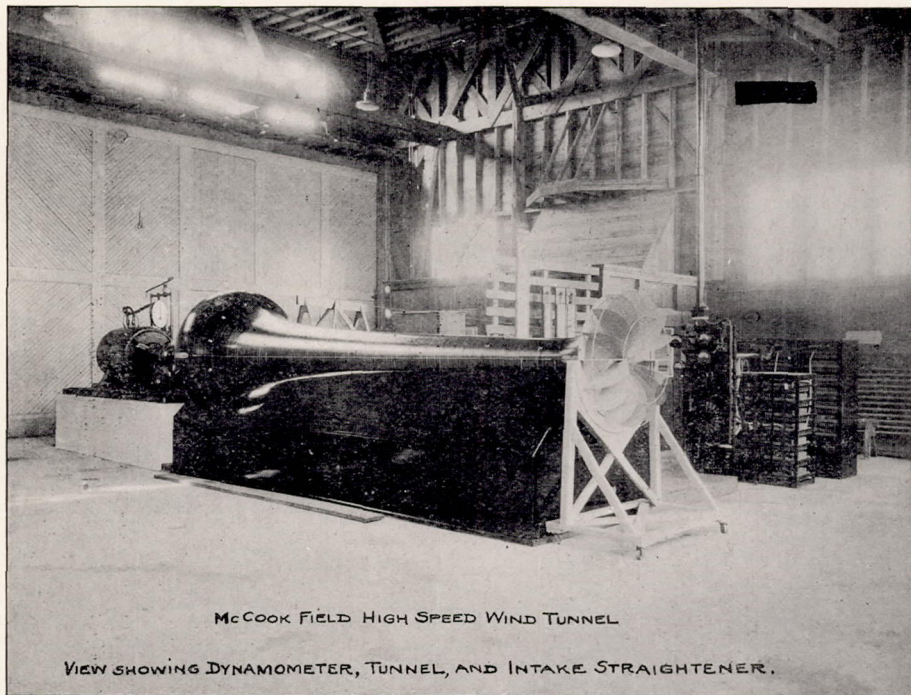


FIG. 12.

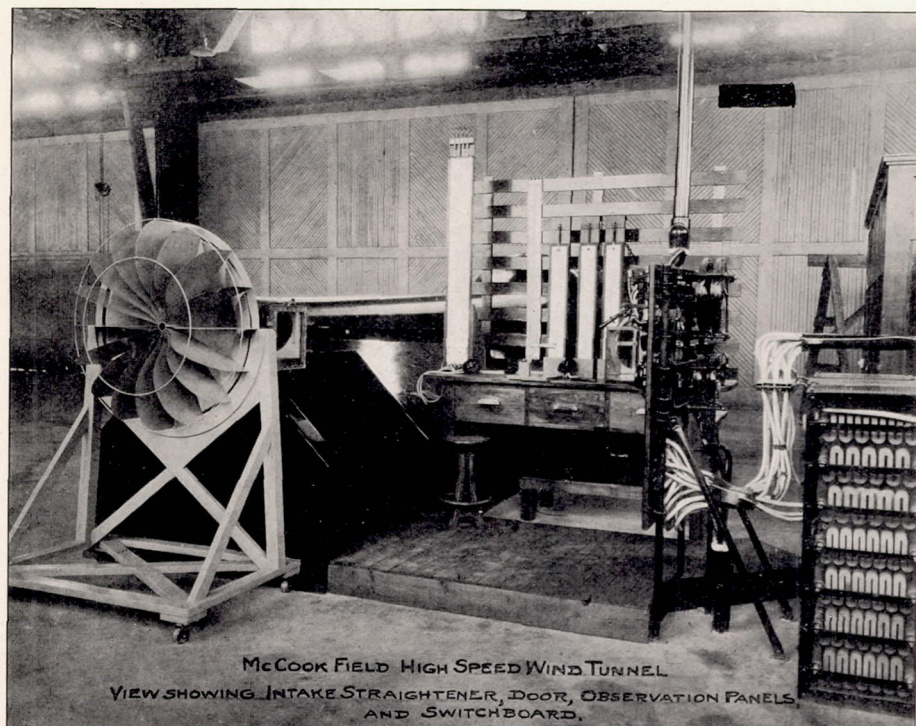


FIG. 13.

Performance of McCook field venturi wind tunnel; no straighteners.

(Barometer, 29.55 inches Hg. Room, 62° F. Density, 0.0755 lb./ft.)

Tunnel speed.	Fan speed.	Torque, 63-inch arm.	Horse-power.	Difference at choke.	Inches of water, center section.			Inches of water, exit section.			Ratio of static suction.	
					Static.	Impact.	Difference.	Static.	Impact.	Difference.	Choke to center.	Choke to exit.
<i>Mi./hr.</i>	<i>R. p. m.</i>			0.306	0.07	0.00	0.07	0.07	0.13		4.28	
25	120			1.22	.29	.03	.26	.20	.23		4.21	
50	205			2.76	.65	.20	.45	.50	.50	0.06	4.245	
75	305	2.0	0.61	4.91	1.20	.10	1.10	.90	.70	.20	4.09	
100	425	5.2	2.21	7.67	1.70	.20	1.50	1.25	1.00	.25	4.53	6.14
125	510	8.0	4.08	11.03	2.50	.50	2.00	1.90	1.60	.30	4.42	5.80
150	610	13.0	7.93	15.02	3.15	.70	2.45	2.30	1.90	.40	4.77	6.53
175	675	16.4	11.07	19.63	4.50	.50	4.00	3.20	2.00	1.20	4.36	6.14
200	800	23.5	18.80	24.86	5.60	.50	5.10	3.90	2.70	1.20	4.44	6.37
225	880	29.5	25.95	30.70	6.60	.60	6.00	5.00	3.00	2.00	4.60	6.07
250	990	37.0	36.63	37.15	8.00	1.00	7.00	6.00	4.50	1.50	4.645	6.19
275	1,090	45.0	49.00	44.20	9.50	2.00	7.50	7.70	5.70	2.00	4.652	5.74
300	1,220	56.0	68.30	51.80	11.00	3.00	8.00	8.70	5.70	3.00	4.72	5.95
325	1,290	63.0	81.20	60.10	13.00	3.00	10.00	10.10		7.00	4.625	5.95
350	1,390	72.0	100.00	78.60	16.00	4.00	12.00	12.20		9.00	4.915	6.44
400	1,550	93.0	144.20	106.60	21.00			16.50			5.07	6.46
465	1,770	110.0	194.60								5.10	6.15

¹ Average.

	Diameter.	Area.		Distance from choke.
	<i>Inches.</i>	<i>Inches.²</i>	<i>Feet.²</i>	<i>Inches.</i>
Choke.....	14.000	153.94	1.068	0
Center.....	22.375	393.20	2.732	100
Exit section.....	47.250	1,753.50	12.180	190

The net blade discharge area is 8.38 square feet, which is 7.84 times the area of the choke. With a choke speed of 100 miles per hour, air was noted to leave the propeller at an angle of 45° with the plane of the fan and at an angle of 15° radially from a tangent. The component velocity was noted to be about 47 miles per hour. The average ratio of choke to exit suction throughout the above range from 25 to 465 mi./hr. is 6.5.

NOISE.

Careful study of fan and cone design results not only in reduced losses but also in reduced noise. In the past the noise has been a serious objection to speeds greater than 70 miles per hour in wind tunnels. It may be said that 60 per cent of the roar of any airplane is due to the propeller. For wind tunnel use, the combination of fan and cone adopted has brought about a considerable improvement, as indicated in the following tabulation:

From the operator's position:

The fan is noiseless at.....	50
The fan starts to roar at.....	60
Conversation is easy at.....	125
Conversation is slightly forced at.....	155
Conversation is possible 12 inches apart at.....	240
Conversation is possible at 4 inches apart at.....	300

PRECISION.

The precision of wind-tunnel work in general is dependent in the last analysis upon the velocity readings. By means of adopting the instantaneous reading method, however, the inaccuracies usually to be expected due to velocity fluctuation have been greatly decreased, as was shown at the start of the experiments by study of the velocity graphs. The method was found normally to be very satisfactory, but under abnormal conditions, as for instance when the doors were open and the wind was blowing outside, the tests became impracticable.

The precision of any one reading depends upon the skill of the observers and on the amount of time at their disposal for identifying the fluctuations of their respective instruments. The individual readings of the tests here reported have precision slightly less than could be obtained in the conventional wind tunnel where a honeycomb is used; hence the desirability of a plurality of observations at small velocity increments. The results as plotted show the same order of precision as is reached in the conventional wind tunnel. Moreover, scaling effect of experiments so far exceeds the degree to be predicted from past knowledge of the $\frac{LV}{\nu}$ ratio, that it is not found necessary to question the adequacy of the precision.

In general no difficulty was encountered in checking a given run with different crews and on different days.

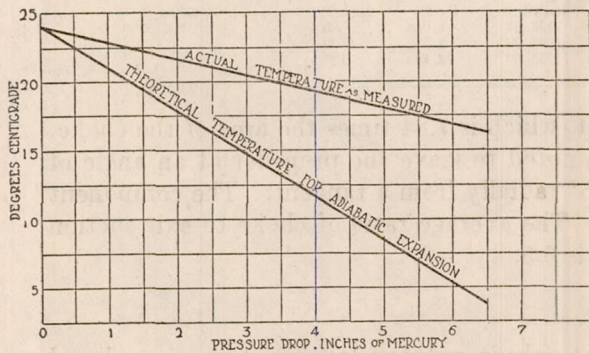


FIG. 17.

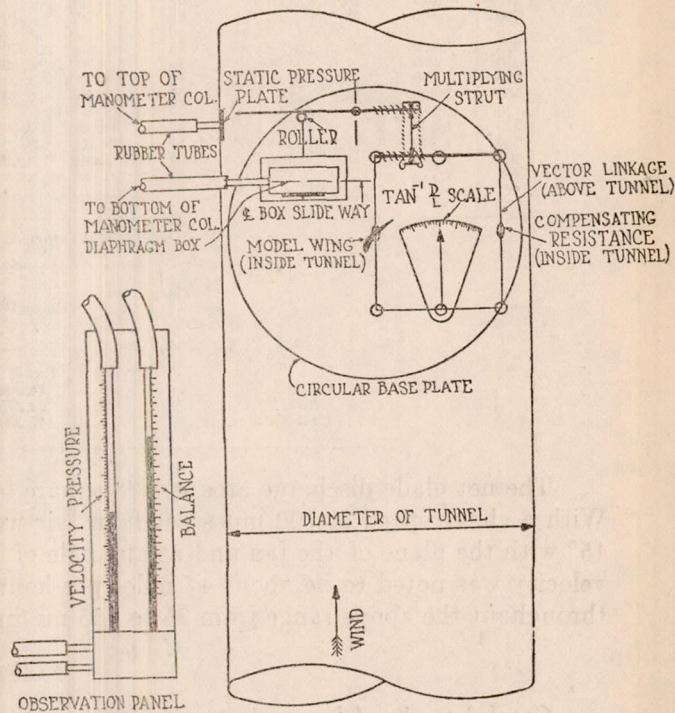


FIG. 18.

The determination of true velocity is dependent upon a knowledge of the temperature and density of the air flowing through the observation section. The temperature is calculated on the assumption that the expansion is adiabatic from the atmospheric pressure to the pressure corresponding to the dewpoint, and is polytropic below the latter pressure. A correct knowledge of throat temperature is, of course, essential; and it is necessary to develop a special method of thermometry for reading it. Present methods are inapplicable to its direct measurement, for a thermometer introduced into the air stream occasions more or less adiabatic compression of the air striking it, with consequent rise of temperature at the point of impact. (See chart, fig. 17.) The most advantageous position for the thermometer is with the bulb downstream, where it is subject chiefly to skin friction rather than impact. Further investigations are being made of the matter.

For the graphs of this report the usual wind-tunnel practice has been followed, wherein the density in the room rather than in the tunnel is used as a basis on which to figure velocity. This has been done for convenience in view of the complicated laws which govern the density of the air in the tunnel itself. The correction when applied does not change the value of the lift coefficient, but changes the corresponding value of the velocity.



FIG. 18½.--TRANSITION TYPE OF AIR FLOW ABOUT AEROFOIL AT SECOND CRITICAL SPEED (LOOKING ALONG AXIS OF TIP VORTEX).

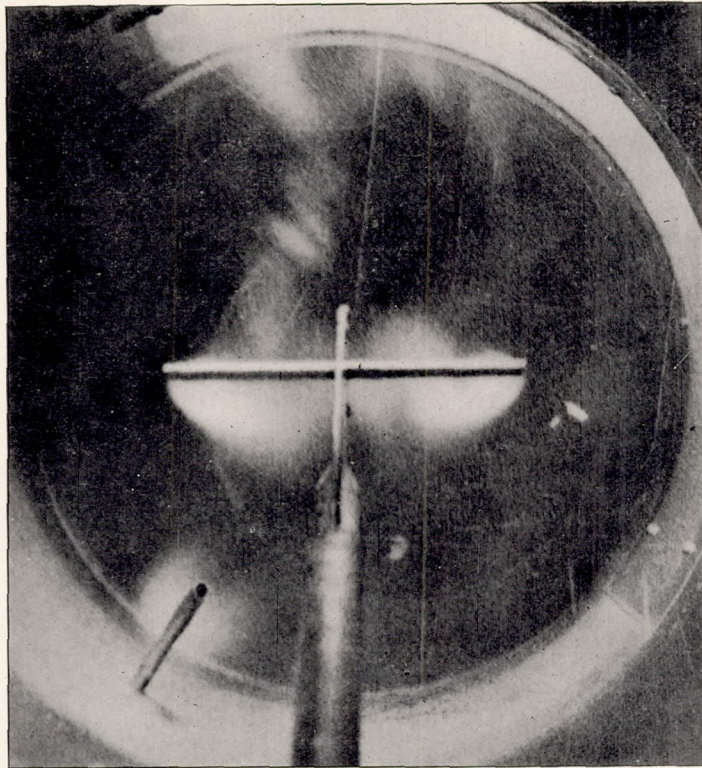


FIG. 19.—AIR FLOW IN TRANSITION STAGE BETWEEN HIGH AND LOW LIFT RÉGIME.

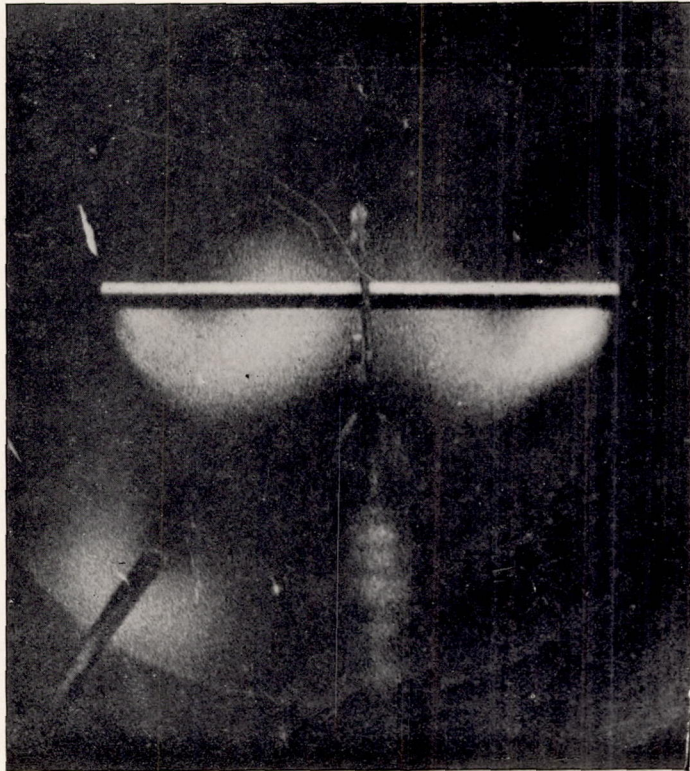


FIG. 20.—FLOW CORRESPONDING TO HIGH LIFT RÉGIME. STABLE UP TO THE CRITICAL SPEED.

It might be desirable to explain how the lift coefficient is calculated, so that it will be apparent that the density does not enter into the calculation. Suppose that h represents the height of the water column corresponding to the velocity head at a velocity V ; then, if $\frac{\rho}{g}$ represents the density of the air in slugs, $\frac{\rho}{g} \times V^2 = K_1 h$

If P represents the lift on the model, and A its area, and K_y the absolute lift coefficient, then—

$$P = K_y \frac{\rho}{g} A V^2, \text{ and } K_y = \frac{P}{\frac{\rho}{g} A V^2}$$

Substituting,
$$K_y = \frac{P}{A K_1 \times h}$$

It is evident that this last expression is independent of density, and as this equation is used in calculating the value of the lift coefficients in all cases, the density of the air in the tunnel does not affect the value of the lift coefficient.

METHOD OF SUPPORTING THE AEROFOIL.

The effect of the center support on the lift coefficient is not considered serious. This conclusion is based on experiments run at other laboratories where the effect of the support has been carefully determined; also on a comparison of the present series of experiments with tests made elsewhere on a larger model supported at the end, for the same VL values. The effect of the center support on drag, however, is known to be very large, so that the results on drag have not been given except in a qualitative way.

The one-end spindle used at the National Physical Laboratory can not be utilized under the conditions of these tests. In order to definitely delimit the effect of the supporting member, further developments are proposed wherein this effect will virtually be eliminated from the tests.

VISUALIZATION OF FLIGHT VORTICES.

The method of visualizing air flow, discovered by the writers together with C. P. Grimes, offers a solution to one of the fundamental problems of aerodynamics. This problem is the quantitative empirical measurement of the phenomena of fluid dynamics appertaining to flight and air flow.

The accepted theory upon which flight has its physical basis is purely rational. It has not yet been directly applicable to engineering design, because empirical measurement of flight vortices has never been made. Therefore, the aeronautical engineer's use of aerodynamics is largely according to the cut and try method. He can not, on the drafting board, depart from known shapes, speeds, or sizes; should he wish to do so, he must first build a model and determine the coefficients applicable to his new design.

To illustrate this point, it is only necessary to refer to the simplest case, that of an airplane wing. We can measure the coefficient of force on a small model of this wing to an accuracy of 1 per cent. But we do not know definitely how the accuracy is changed by scaling up to full size, or to full speed. We can not, without tests, predict the change of coefficient to be expected when the wing shape is altered, or the angle of attack, or the position with reference to other surfaces.

Aerodynamical theory will serve practical use when supported by empirical data. In the past flight vortices have never been measured, nor even visualized to a usable extent. Analysis of air flow has been confined to the use of smoke or powder set loose in the air to indicate lines of flow; or of threads used as wind vanes. Or we have been driven to analogies derived from study of fluids of differing viscosity and density, such as water. Or, further, we have sought by measurement of static pressures in the air surrounding a body to deduce the lines of flow. But

these methods have given small encouragement toward the practical application of the vortex theory to engineering use.

The method described herewith depends upon the fact that the moisture in the air condenses out as fog when the temperature is reduced to the dew point, provided there is a solid or liquid nucleus to start the condensation. In the McCook Field wind tunnel the temperature drop is brought about through expansion of the air during acceleration due to 100 inches of water suction. Relative humidity of the atmosphere can be artificially raised if too low. The necessary nucleus for condensation is provided by the model itself.

Flight vortices become readily visible and can be photographed with the aid of searchlights. Several efforts were made to take the pictures with a plate camera, but these were not very successful. Finally a good moving picture was taken and some of the films enlarged. While these films showed up very well on the screen the detail was not very clear in enlargement, so that in addition to the searchlights, which were provided with nitrogen-filled incandescent lamps, two carbon arc lights were set up in order to give a greater amount of blue light. The results obtained from the motion-picture camera with the carbon arc lighting were fairly satisfactory, and a number of enlargements from the motion-picture films are reproduced in this paper. Figure 21 is an enlargement of a moving-picture film looking downstream. It is inferior to visual observation, the vortices showing as below the model, due to parallax. To the naked eye they are in line with the wing tips and are clean-cut, perfect circles. They extend downstream a distance of several dozen chord lengths from the rear corner of each wing tip, enlarging in diameter as the distance increases, and converging slightly in the horizontal plane. (See figs. 1 and 30.) In the vertical plane the tip vortex axis takes a decided downward angle, intermediate between the horizontal and the line of travel of the flat sheet of edge vortices.

NOTE.—For an excellent mathematical discussion of the shape and arrangement of the tip vortices and the trailing vortices see Report No. 28 of the National Advisory Committee for Aeronautics (United States). On page 44 the author, Dr. George DeBothezat, has given some sketches, figures 38 and 39, which show in an interesting way that the axis of the tip vortices is intermediate between the direction of movement and the sheet of trailing edge vortices.

For corroboration of the vortex phenomena at slow speeds where condensation is not visible, steam jets have been useful. When of proper saturation, such a jet introduced in the tunnel intake provides a good indication of the flow lines, and is superior to the conventional smoke jet.

Adequate analysis of the flight vortices will be made in future with special apparatus at present under consideration. The shape, size, and direction of the tip vortices can be easily noted and seem fairly susceptible of measurement. The periodic run of the edge vortices is too quick for recognition by the naked eye or even for identification by the moving-picture camera; it requires stroboscopic analysis.

The observed vortices differ for different aerofoil set-ups and different speeds. For instance the observed tip vortex at 18° has less than one-half the diameter manifest at 8° , while the line of edge vortices is less noticeable at 18° .

Again, the character of the general vortex phenomenon undergoes remarkable change at the critical speed. In the high-lift régime the general shape is like a trough whose floor (edge-vortex sheet) slopes downward from the trailing edge and whose walls (tip vortices) are increasingly high as the distance downstream increases. The cross section is roughly like a shallow U.

At higher speeds, however, in the low-lift régime the observed phenomenon is suddenly altered. Following out the above homely analogy, we may imagine that the "walls" of the trough remain substantially as before. The "floor," however, splits longitudinally, curls upward, and extends the two limbs, now free, to a point well above the level of the tip vortices. Figures 26 and 2 are enlargements of two motion-picture exposures which were intended to record the sequence of the change. These photographs are not altogether satisfactory, and are therefore supplemented by the two sketches of figure 34.

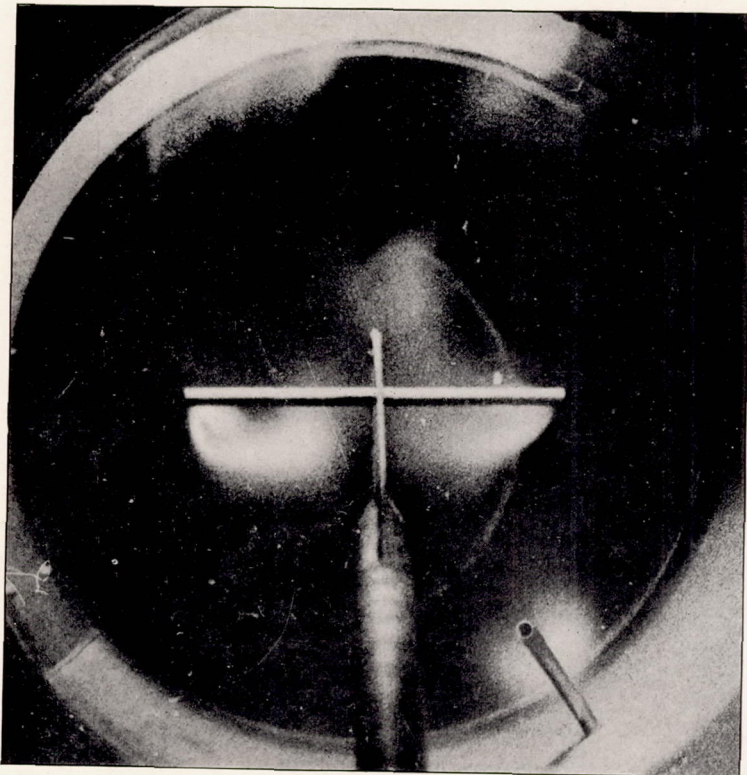


FIG. 21.—ON THE RIGHT SIDE THE FLOW HAS GONE OVER TO THE INEFFICIENT TYPE. THIS IS STABLE AT SPEEDS HIGHER THAN THE CRITICAL SPEED.

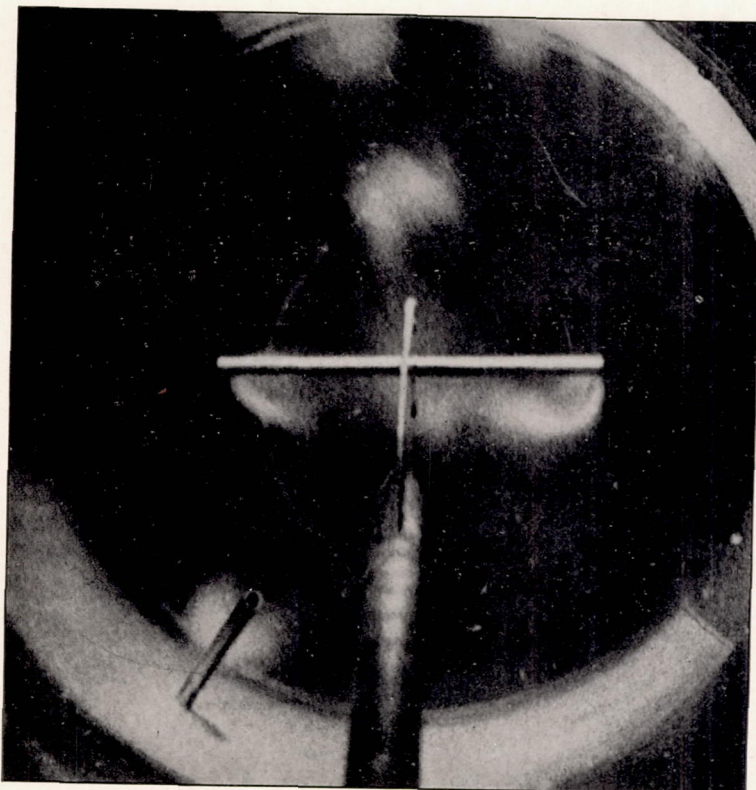


FIG. 22.—THE MODEL SUPPORT HAS BEEN MOVED OUT OF LINE WITH THE TUNNEL AXIS TO MAKE ROOM FOR THE CAMERA.

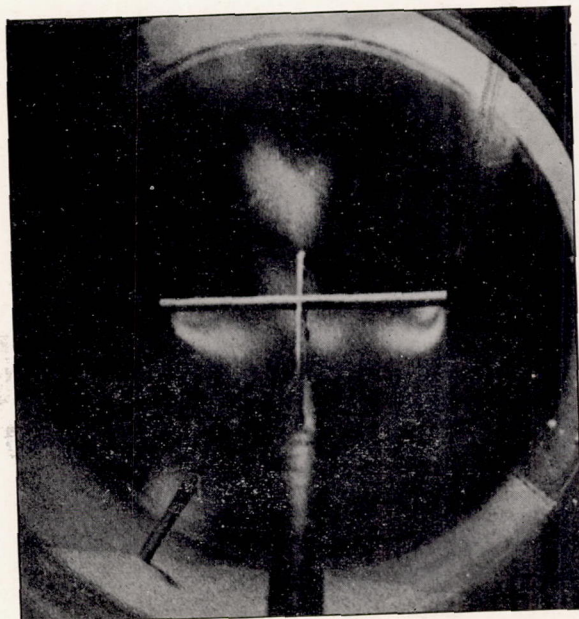


FIG. 23.—AIR FLOW AT SECOND CRITICAL SPEED. NOTE THE DISTURBANCE BEHIND CENTER OF AEROFOIL, CAUSED BY SUPPORTING ROD.

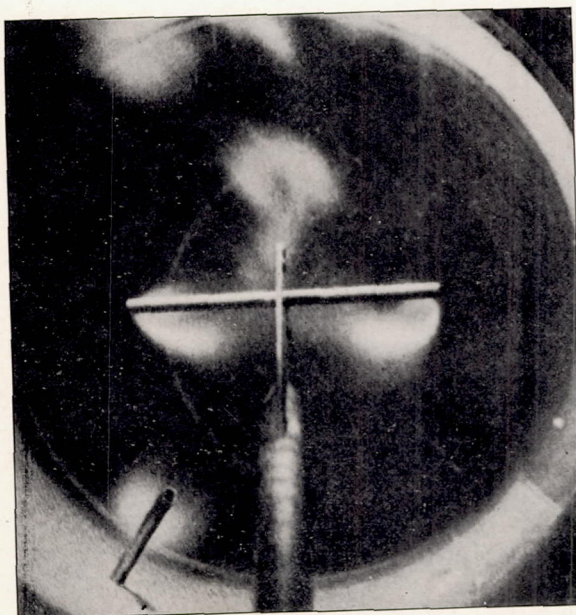


FIG. 24.—IN THIS PICTURE THE DISTURBED AIR FLOW BEHIND THE SUPPORT HAS TAKEN A DIFFERENT SHAPE. NOTE TENDENCY TO MERGE WITH DISTURBANCES AT PERIPHERY OF TUNNEL.

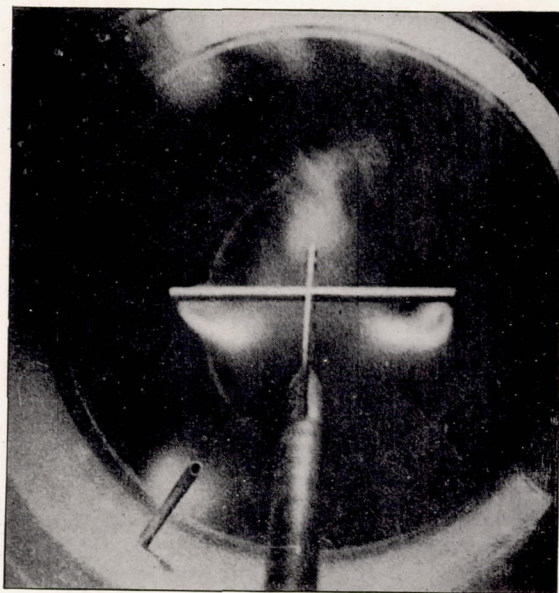


FIG. 25.—DARK CENTER OF RIGHT TIP VORTEX SHOWN IN PERSPECTIVE.

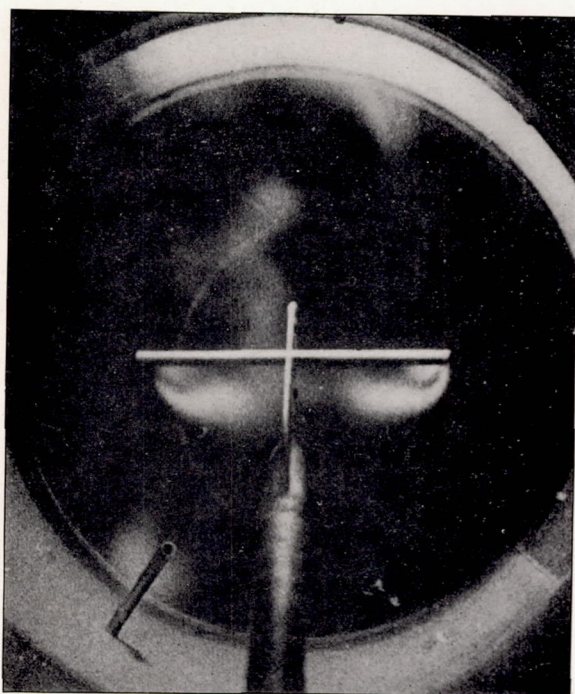


FIG. 26.—LOW LIFT RÉGIME ON LEFT HALF SPAN; HIGH LIFT ON RIGHT.

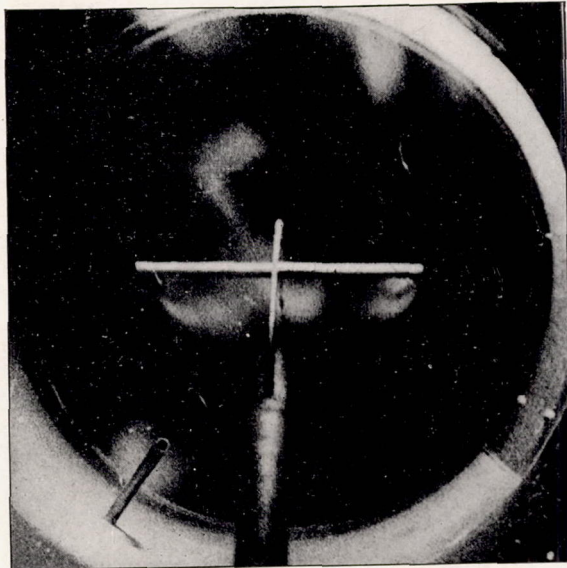


FIG. 27.—THIS EXPOSURE IS ADJACENT IN THE CINEMA FILM TO THAT OF FIG. 26.

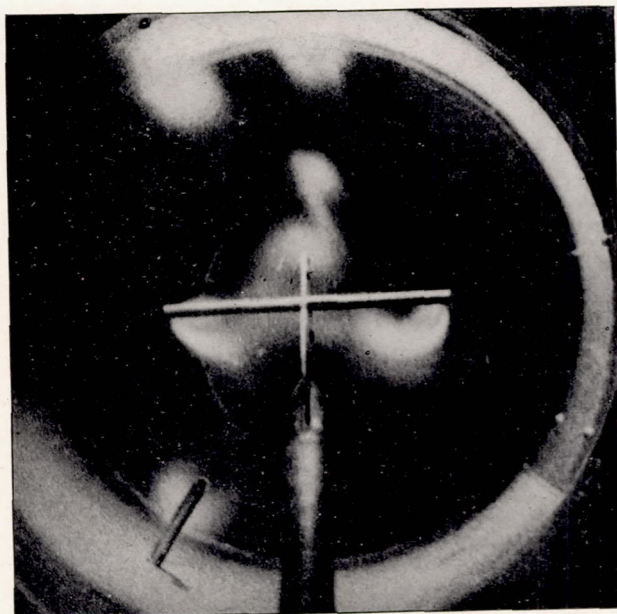


FIG. 28.—THE DISTURBANCE BEHIND THE CENTER SUPPORT SHIFTS BACK AND FORTH VERY RAPIDLY AND AT THE SAME TIME CHANGES ITS SHAPE.

The shape and movement remind one in a striking manner of the lightning observed when electrical discharges take place in the sky.

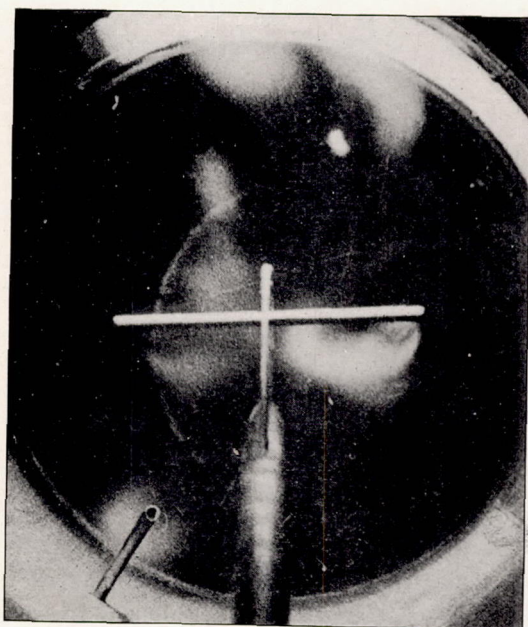


FIG. 29.—UNSYMMETRICAL CONDITIONS OF AIR FLOW ON THE TWO HALF SPANS.

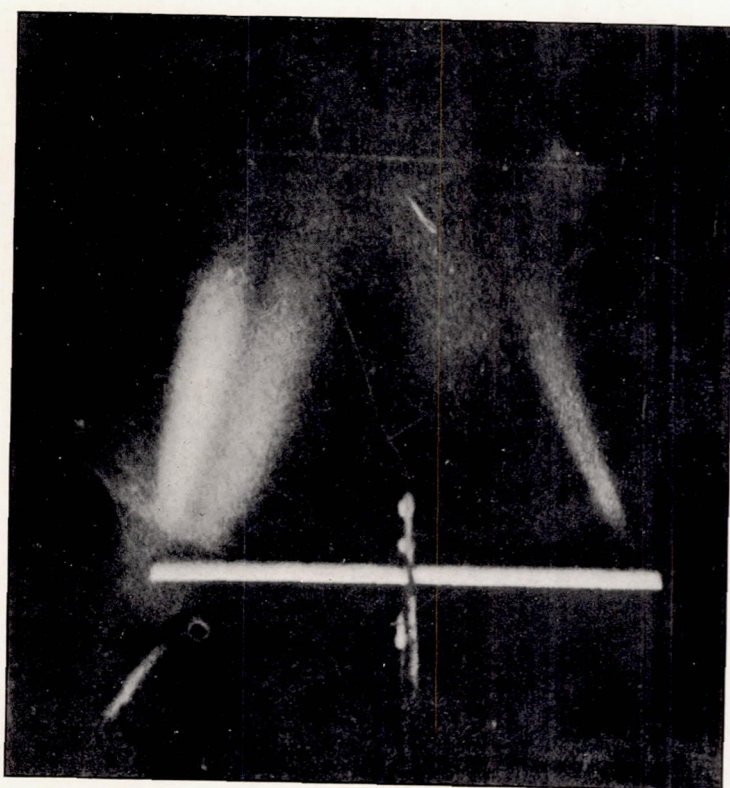


FIG. 30.—VIEW FROM ABOVE THE MODEL; LINE OF SIGHT ABOUT 30° FROM LINE OF FLOW.

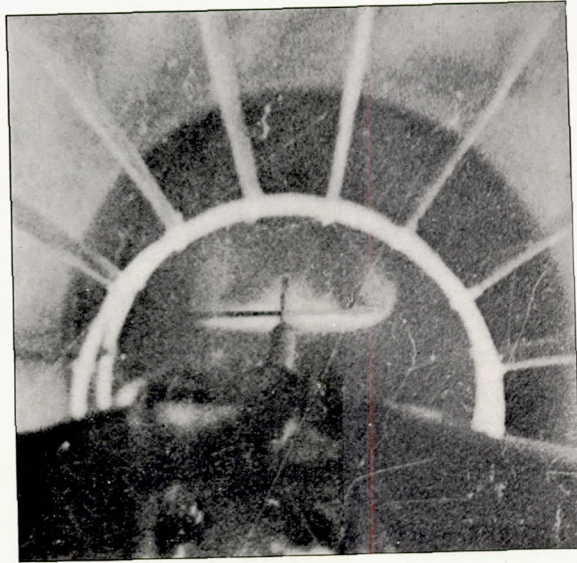


FIG. 31.—EFFICIENT TYPE OF FLOW STABLE AT LOW SPEEDS.

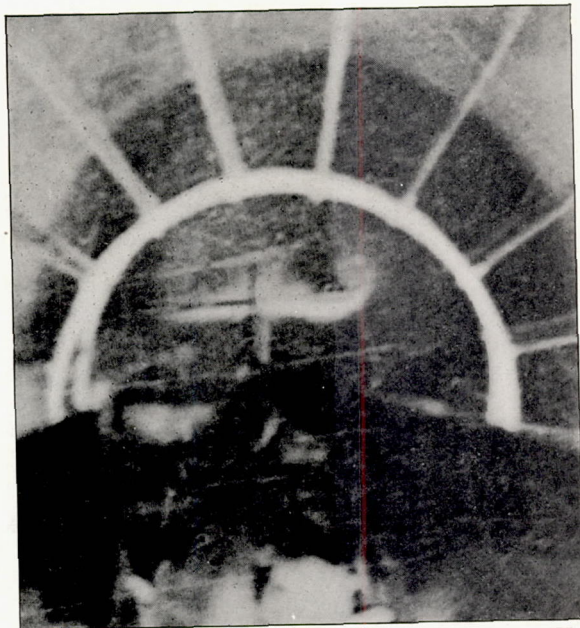


FIG. 32.—UNSTABLE FLOW OCCURRING ONLY AT THE CRITICAL SPEED.

Note the cusp halfway out the right wing.

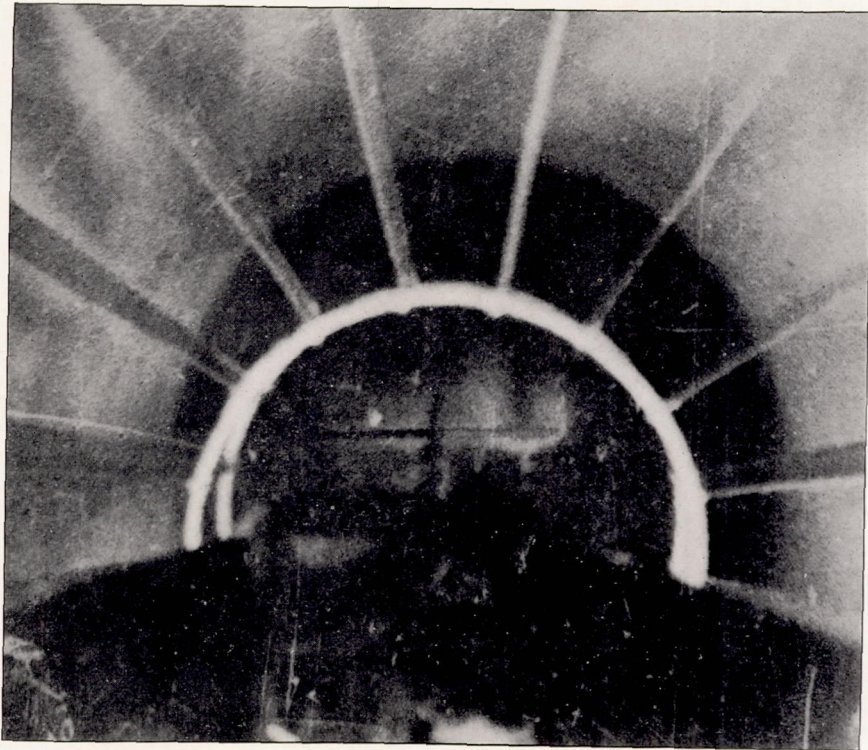


FIG. 33.—INEFFICIENT TYPE OF FLOW, STABLE AT HIGH SPEEDS.
Note the stream extending vertically upward halfway out the right half span.

Figure 34-a is a diagram of the end view of the high-lift phenomenon as it appears distinctly to the naked eye. The right-hand side of the aerofoil in figure 26 approximates this condition, the left-hand side having already gone over to low-lift flow. Figure 34-b is a diagram of the low-lift phenomenon; the left-hand side of aerofoil in figure 2 shows this fairly well, the right-hand side being in a transition stage. Figure 33 shows the low-lift flow better than figure 2, but is dim. Figure 1 is a three-fourths view of the low-lift flow, and also represents other features mentioned above.

An interesting variation of the flight vortices is furnished by replacing the aerofoil by a flat disk normal to the wind. Here the phenomenon can be seen as a "streamline" fog surface, converging toward a point half a dozen diameters downstream.

Figure 19 illustrates the distance above the aerofoil to which the flight vortex phenomena may extend and shows their tendency to merge with other whirls attributable to the wind tunnel walls. The extent of the phenomena may be four or more chord lengths above the aerofoil; this further develops investigation made by the writers in 1911, when it was shown experimentally that the air flow above a wing is disturbed to a distance of at least four chord lengths. (See "The Center of Pressure Travel on Airplane Surfaces and Birds' Wings," Mass. Inst. of Technology, 1911.)

Reference is also made to the work of J. R. Pannell, dealing with experimental evidence as to the extent of circulation about an aerofoil.

VISUALIZATION OF UNOBSTRUCTED AIR FLOW.

When the model is removed the vortices and eddies of flow through the unobstructed throat may be observed by looking into the intake or through the transparent shield of the observation section. The condensation is more pronounced behind the impact tube and thermometer bulb than elsewhere, since these are obstacles to the flow and therefore constitute nuclei for condensation. A projecting cotter pin one-sixteenth inch high at the wall causes a perfect vortex, which shows up against the white foggy background as a black circle.

The general appearance of the air flow, which may be considered typical of all air flow, is as follows: A cross section at the throat shows a seething mass of fog specters, denser at the walls than at the center, though occasionally the entire disk fills up with fog to the point of opaqueness. The specters have in the cross-sectional plane a gentle movement like the flame of an alcohol stove, showing the constant readjustment of equilibrium. Vortices and S-shaped whirls continually form and, after moving about, lose themselves in the general confusion. In a diagonal view they take the appearance of long, foggy fibers, stretching down the tunnel like wooden moldings. The axes of whirl are, of course, longitudinal. Under proper humidity and lighting conditions the whole becomes a beautiful iridescent sight, violet and purple hues predominating.

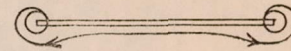


FIGURE - 34-a

HIGH LIFT REGIME

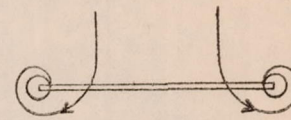


FIGURE - 34-b

LOW LIFT REGIME

FIG. 34.

Figure 1-a is a diagram of the end view of the high-speed phenomenon as it appears in the right-hand side of the tunnel in figure 2b approximately the same distance from the right-hand side of the tunnel as the flow in figure 2a. Figure 2a is a diagram showing the left-hand side of the tunnel in figure 2b. Figure 2c shows the same flow as in figure 2a but in a transition stage. Figure 2d shows the flow as in figure 2a but in a transition stage. Figure 2e shows the flow as in figure 2a but in a transition stage.

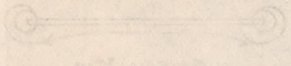


FIGURE 2. (a) Flow in the tunnel. (b) Flow in the tunnel. (c) Flow in the tunnel. (d) Flow in the tunnel. (e) Flow in the tunnel.

The distance between the end-views of the light source is indicated by a horizontal line with arrows at both ends. The distance between the end-views of the light source is indicated by a horizontal line with arrows at both ends. The distance between the end-views of the light source is indicated by a horizontal line with arrows at both ends.

The distance between the end-views of the light source is indicated by a horizontal line with arrows at both ends. The distance between the end-views of the light source is indicated by a horizontal line with arrows at both ends. The distance between the end-views of the light source is indicated by a horizontal line with arrows at both ends.

The distance between the end-views of the light source is indicated by a horizontal line with arrows at both ends. The distance between the end-views of the light source is indicated by a horizontal line with arrows at both ends. The distance between the end-views of the light source is indicated by a horizontal line with arrows at both ends.

THE EFFECT OF THE TUNNEL ON THE FLOW

The effect of the tunnel on the flow is shown in figure 3. The flow is shown as a horizontal line with arrows pointing right. The flow is shown as a horizontal line with arrows pointing right. The flow is shown as a horizontal line with arrows pointing right.

The effect of the tunnel on the flow is shown in figure 3. The flow is shown as a horizontal line with arrows pointing right. The flow is shown as a horizontal line with arrows pointing right. The flow is shown as a horizontal line with arrows pointing right.

REPORT No. 83.

PART III.

MODEL TESTS ON PROPELLER AEROFOILS.

BY F. W. CALDWELL AND E. N. FALES.

The six aerofoils adopted for tests were of 6 inches length, 1 inch chord, and 0.1 to 0.2 camber. The cross-sectional shape, as shown in figure 35, is that upon which the engineering

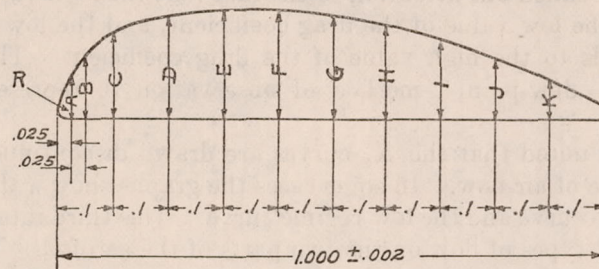


FIG. 35.

Max. thickness.	A	B	C	D	E	F	G	H	I	J	K	R
0.08	0.032	0.047	0.063	0.076	0.080	0.079	0.076	0.069	0.059	0.044	0.028	0.008
.10	.041	.059	.079	.095	.100	.099	.095	.087	.074	.056	.035	.010
.12	.049	.070	.094	.114	.120	.118	.114	.104	.088	.067	.042	.012
.14	.057	.082	.110	.133	.140	.138	.133	.121	.103	.078	.049	.014
.16	.065	.094	.126	.152	.160	.158	.152	.139	.118	.089	.056	.016
.18	.073	.106	.142	.171	.180	.178	.171	.156	.133	.100	.063	.018
.20	.082	.118	.158	.190	.200	.198	.190	.174	.148	.112	.070	.020

division has standardized for propeller use. As was expected, a broad interpretation of results was facilitated by the diversity of cambers, angles, and speeds available. Thanks to the discovery of the method of air-flow visualization it was possible to give a physical interpretation to the balance readings. In the discussion of results which follows it will therefore be noted that the phenomena will be referred to interchangeably in terms either of vortex formation or of lift-and-drift.

The outstanding conclusion to be drawn from the tests is that we have more than one régime of air flow to deal with in aerofoil study, and that these régimes are separated by conditions of discontinuity. The characteristics usually associated in aeronautical engineering with a practical aerofoil do not apply outside the small range of cambers, speeds, and angles utilized in flight. Beyond this range the flow about the aerofoil no longer produces the familiar results in terms of lift and drag, but becomes analagous to the flow about a body of irregular shape. Efficient lift of an aerofoil is only a single case of several distinct aerodynamic phenomena resulting from air flow past a solid body. When the speed of air flowing past an aerofoil increases there is first a régime of relatively low-lift effect, then at higher speeds an efficient lift effect such as applies in flight, then at still higher speeds a drop back to a second low-lift effect. As the angle or camber increases the high-lift régime becomes discontinuous and is succeeded by the low-lift régime; the transition point is spoken of in conventional graphs as the "critical, or stalling, angle," or the "burble point."

All of the sections show, at certain angles, two speeds at which the flow is unstable and discontinuous. At the point of discontinuity occurring at the lower speed increase of speed shows an increased lift coefficient and a decreased drag coefficient so that the lift-drag ratio is enormously increased. At the point of discontinuity occurring at the higher speed increase of speed shows a decreased lift coefficient and an increased drag coefficient, so that the lift-drag ratio is enormously decreased. Thus these sections have a definite speed range at each angle within which the flow is efficient and produces a high lift-drag ratio and a fairly constant lift coefficient. It may be called the régime of high L/D , and includes the phenomena appertaining to practical flight. This speed range has been definitely measured for the higher angles, but apparently it goes beyond the speed obtainable in the tunnel for the lower angles.

Before this series of experiments was started the attention of the writers was called by Mr. Orville Wright to the fact that he had obtained two distinct values of the lift coefficient and the drag coefficient in testing certain aerofoils at certain angles of attack and constant speed. Mr. Wright also called our attention to the fact that the high value of the lift coefficient always corresponds to the low value of the drag coefficient, and the low value of the lift coefficient always corresponds to the high value of the drag coefficient. The two values are now clearly proved by the "dew-point" method of observation to represent distinctly different types of flow.

It will therefore be noted that the K_y curves are drawn discontinuous to correspond with discontinuity in the type of air flow. In some cases the graphs show a third curve intermediate between the high-régime curve and the low-régime curve. This third intermediate line undoubtedly represents different types of flow on the two parts of the aerofoil. This is possible because of the center support which divides the aerofoil into two parts. At the point of discontinuity corresponding to the second critical speed the lift reading becomes unsteady; the flow phenomena become unstable and jump from one type to another, until the new form is established. Figures 2, 19, 23 show the unstable flow of the transition, figures 33 and the left side of 25 show the flow of the final low-lift régime.

The discovery of this second critical speed is one of the novel and significant features of the experiments. Simultaneous observation of the balance and of the flight vortices made the discovery possible, affording proof that the two types of flight vortices can be identified with the two values of the lift coefficient, one belonging to a high L/D régime, the other to a low L/D régime.

With the general remarks above it is now proper to make a detailed study of the characteristics of the various curves submitted in this report. The three variables are (1) angle of attack, which is defined as the angle between the flat undersurface of the aerofoil and the direction of the wind; (2) camber, that is, the maximum thickness of aerofoil divided by the chord; (3) velocity, which is given in miles per hour and refers to pressures and temperatures of standard air. It must be understood that all these three factors of angle, camber, and speed affect the régime of air flow, and it is insufficient to explain the air flow régimes in terms of either factor separately from the others. With this reservation certain analyses are given herewith as to the various effects of these factors. Refer to figures 36 to 41.

The effect of the three factors in determining whether the low or high lift régime obtains is shown by the following three examples:

1. As example of angle change, compare the 0.12 camber aerofoil at 17° and 20° ; the high K_y régime does not appear for 20° .
2. As example of camber change compare the 0.10 camber aerofoil with 0.18 camber at 15° , the former case showing high-lift régime, the latter case showing low-lift régime. It must be kept in mind that the unit of "angle" is an arbitrary one, and for its proper definition must depend upon the camber; hence, it is to be expected that the effect of angle and camber changes will be analogous.
3. As example of velocity change, see 0.12 camber aerofoil at $+17^\circ$; it shows high K_y only at intermediate velocities.

Effect of Angle.

The effect of change in angle may be studied in terms of the slope of the K_y -angle curve. For low velocity all cambers show flat curves at the larger negative angles; for high velocity flatness occurs beyond the burble point. As the speed is increased there is a general tendency for the slope of the K_y -angle curve to become less. This is more marked the thicker the section tested, until finally the section having a camber ratio of 0.2, when run at the speed of 450 miles per hour, shows practically no variation in lift coefficient between the angles of -8° and $+10^\circ$. The lift on this section is therefore nearly independent of the angle of attack between the angles of -8° and $+10^\circ$ at this speed.

The slope is greatest where the régime of high K_y values obtains, namely, in the angles of the flight region. The slope is small, and in general positive, at high negative angles and at positive angles beyond the burble point. Negative slopes are not general. It seems that the conventional practice of plotting K_y -angle curves beyond the burble point as continuous curves of negative slope is unjustified, in view of the discontinuity evidenced after the burble point has been reached.

Effect of Camber.

Within the limits observed, K_y increases with the camber up to the burble point, after which it decreases.

Effect of Speed.

Speed change has an effect which is more prominent for the larger cambers than for the small. The effect of speed change on the K_y -angle curves is prominent at small negative angles, where the slope is greater as the speed is less. As a corollary to this it may be noted in general that within the limits observed, the K_y -speed curves approach zero at great speeds.

Maximum value of K_y .

The maximum attainable value of K_y seems limited, no matter what combination of speed, angle, and camber we choose. Thus the highest K_y (0.65) is reached in the 0.14 camber aerofoil at 15° and 150 miles per hour. The lowest (-0.19) is reached in the 0.12 camber at -10° and 50 miles per hour. The 0.10 camber was not tested at a greater negative angle than -8° . Had the tests on this section been carried to -10° it would have shown a lift coefficient algebraically less than -0.19 . Study of this lowest value can be completed only when a flat-plate experiment shall be added to the series. (The negative angles give the equivalent of an aerofoil having flat upper surface and convex under surface.)

Shift of the Angle of Zero Lift.

One of the interesting discoveries of these tests is the shift of the angle of no lift with speed. This is not so noticeable in the thinnest section, where the change is only about 3° between speeds of 50 and 450 miles per hour. The shift is progressively greater with the thicker aerofoils, however, until in the case of the aerofoil with 0.2 camber the angle of zero lift shows a change of about 18° between speeds of 50 and 400 miles per hour.

As the velocity approaches zero the angle at which the lift coefficient is zero appears to approach zero degrees as a limit.

PRACTICAL SIGNIFICANCE OF THE RESULTS.

This no-lift angle shift is significant, as regards experimental no-thrust pitch. A number of model propeller tests have shown this no-thrust pitch to increase with the speed. It is understood that the experimental no-thrust pitch of a propeller does not correspond to the pitch at which the sections are striking the air along the line of zero lift. The two, however, are rather close together as far as the angle of attack is concerned and the shift of the angle of zero lift explains the change in experimental pitch very well.

These tests have at the outset proved useful in clearing up certain problems in propeller design. A practical example concerns the design of the reversible propeller, where the aerofoil in reverse position has to work at a negative angle of attack. Reference to the lift coefficients for the 0.12 camber aerofoil show that at a velocity of 450 miles per hour this aerofoil has very little negative lift, K_y being about -0.1 at an angle of -12° from the chord. It would obviously be impossible to get much thrust out of an aerofoil of this kind in a reverse position. In order to have a satisfactory thrust it is apparent that the aerofoil must be modified in such a way as to depart from the flat underface.

The discovery of the critical speed of these aerofoils has an interesting bearing on the possibilities of high-speed propellers.

We have found by practical experience that if we do not go below a value of V/ND of 0.65, we get a very fair propeller efficiency. As we have gradually increased the speed of our planes we have gone on increasing the revolutions per minute of the engine and the diameter of our propellers so that the value of V/ND has remained about the same for the great majority of propellers in actual service.

We have always assumed that there was no limit to this development aside from the characteristics of the plane and engine. That is, we have made the assumption that we could double our propeller speed just as soon as we were able to double our plane speed and strengthen our engine enough to stand the stresses involved.

It now appears, however, as though there is a limit to propeller speed aside from the value of V/ND , or, to use more familiar terms, aside from pitch ratio.

Unfortunately, even the speed obtainable in the McCook Field wind tunnel is not great enough to measure the limiting velocity for relatively thin sections when set at low angles. Consequently we are only able to infer that it exists from extrapolation of the curve of critical speeds.

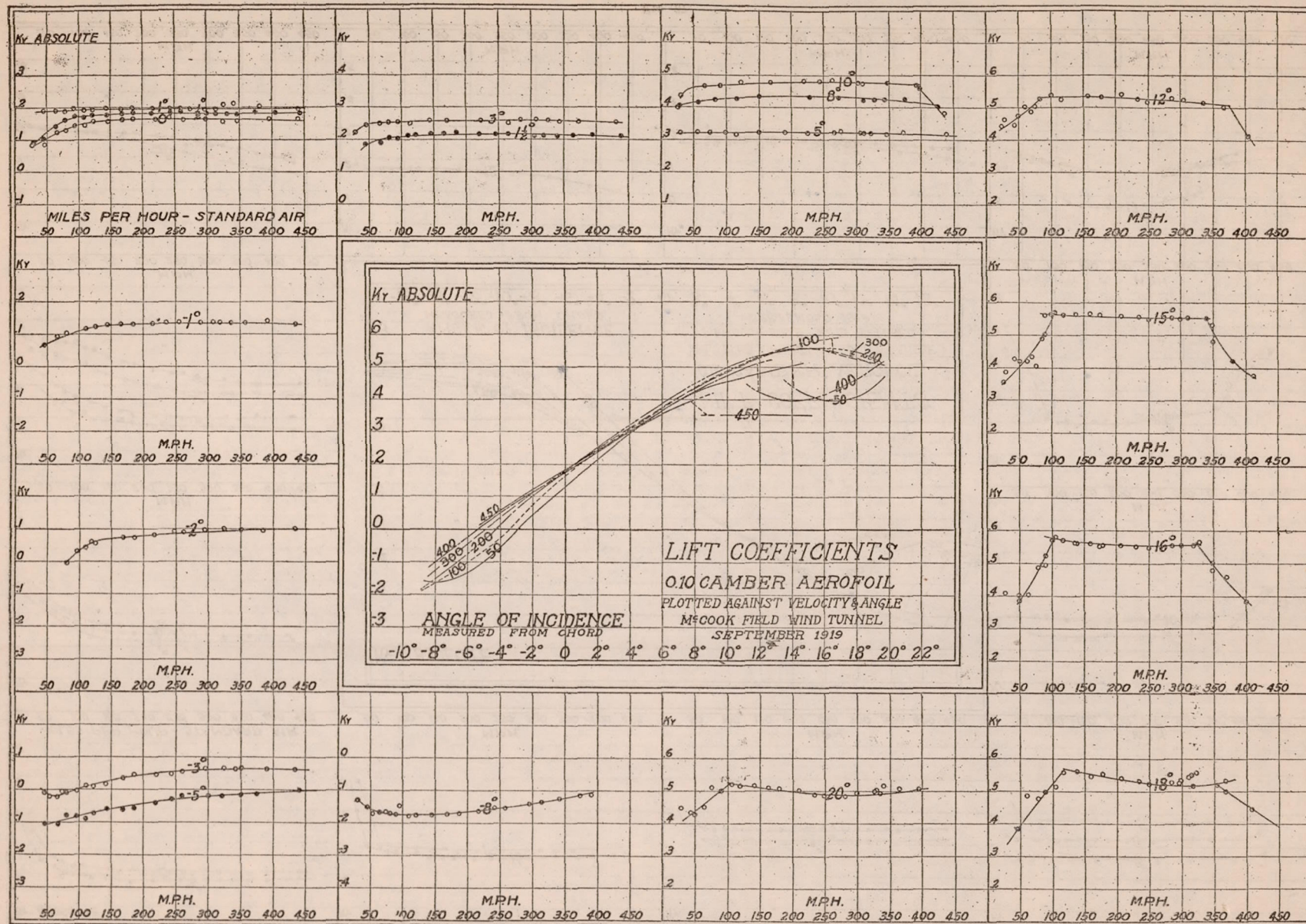


FIG. 36.

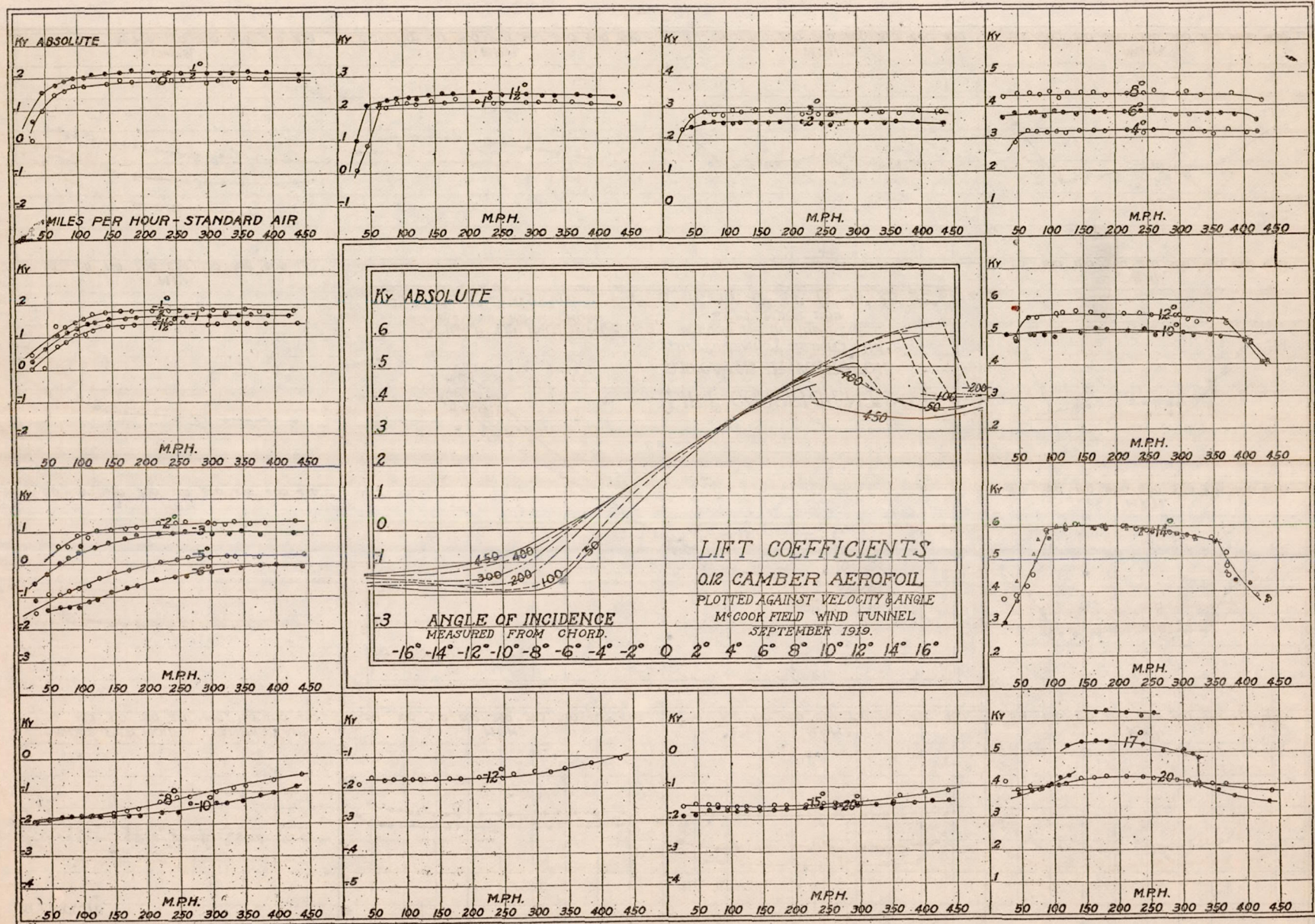


FIG. 37.

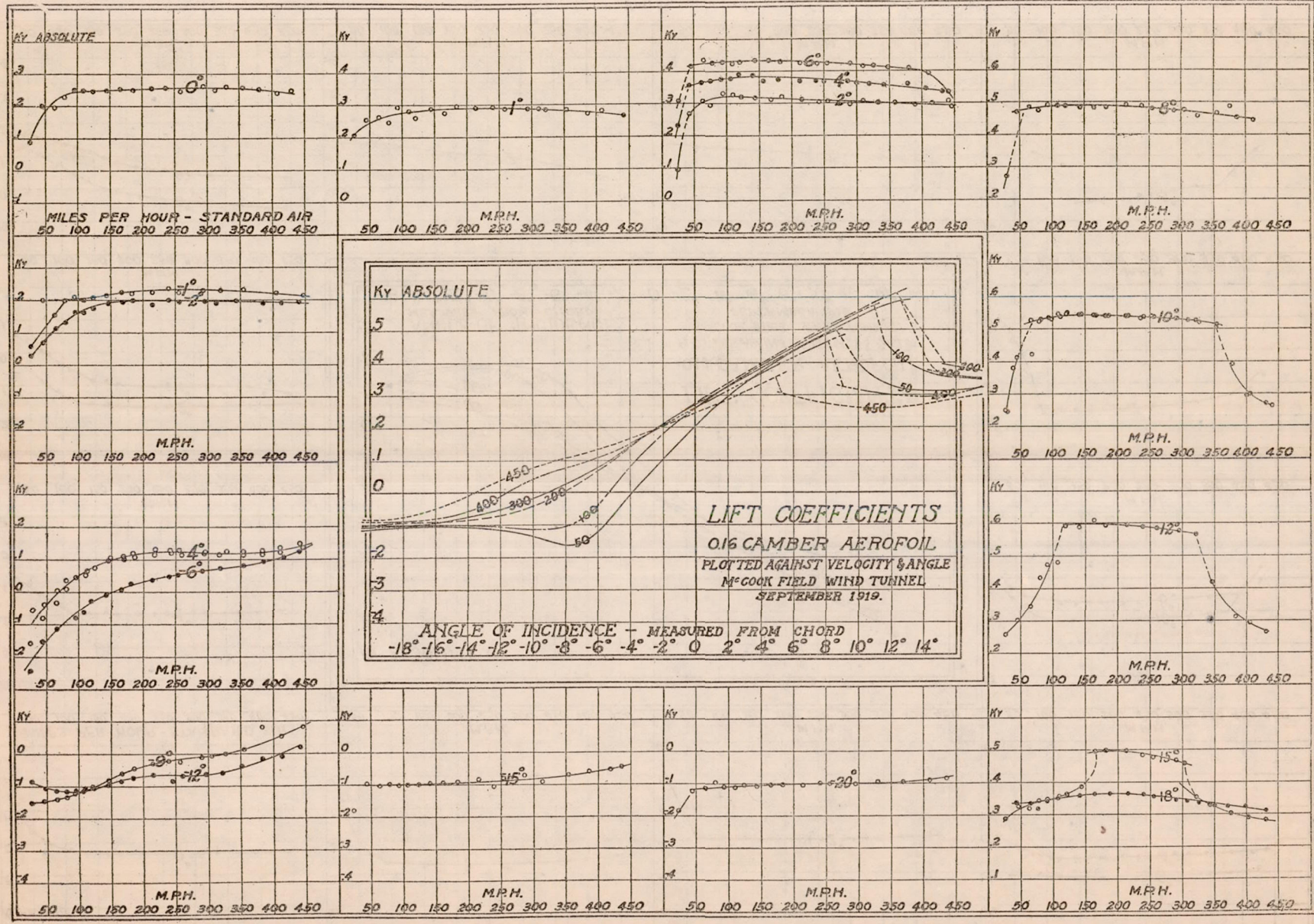
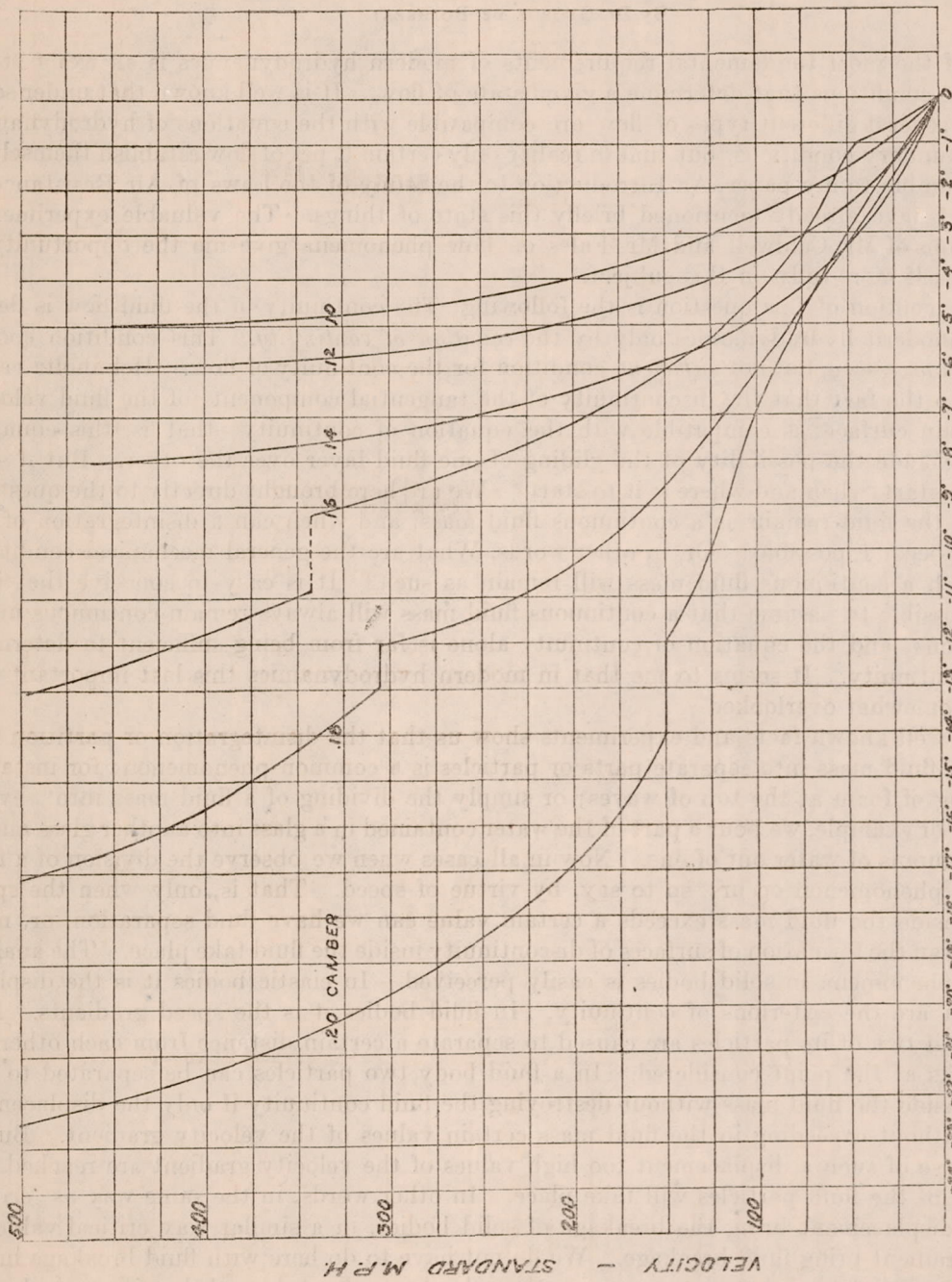


Fig. 39.



ANGLE OF NO LIFT

FIG. 42.

NOTE 1.

A FUNDAMENTAL PROPERTY OF VISCOUS FLUIDS.

By Dr. GEORGE DE BOTHEZAT.

One of the most fundamental requirements of modern hydrodynamics is an exact statement of the conditions that determine a given state of flow. It is well known that under some conditions several different types of flow are compatible with the equations of hydrodynamics and the boundary conditions, but that in reality only certain types of flow establish themselves. In the preamble to my paper, An Introduction to the Study of the Laws of Air Resistance of Aerofoils,¹ I have already mentioned briefly this state of things. The valuable experimental investigations of Mr. Caldwell and Mr. Fales on flow phenomena give me the opportunity to explain myself more fully on this subject.

My conception of this question is the following: The continuity of the fluid flow is determined in modern hydrodynamics only by the *equation of continuity*. This condition constitutes only a *necessary*, but not *sufficient*, condition for the continuity of flow. Helmholtz called attention to the fact that the discontinuity of the tangential components of the fluid velocity along certain surfaces is compatible with the equation of continuity—that is, this equation does not exclude the possibility of the gliding of one fluid layer over the other. But if such gliding can start, when and where is it to start? We are here brought directly to the question, When will the fluid remain as a continuous fluid mass, and when can a disintegration of the fluid mass become possible? Or, in other words, What are the general mechanical conditions under which a continuous fluid mass will remain as such? It is easy to conceive that it is quite impossible to assume that a continuous fluid mass will always remain continuous under all conditions; and the equation of continuity alone is far from being sufficient to determine the flow-continuity. It seems to me that in modern hydrodynamics this last important fact has been somewhat overlooked.

Many well known facts and experiments show us that the disintegration or partition of a continuous fluid mass into separate parts or particles is a common phenomenon; for instance, the forming of foam at the top of waves; or simply the dividing of a fluid mass into several masses. For example, we pour a part of the water contained in a glass into another glass and so get two volumes of water out of one. Now in all cases when we observe the division of a fluid mass, this phenomenon occurs, so to say, by virtue of speed. That is, only when the speed gradient inside the fluid mass exceeds a certain value can we have fluid separation, or, more generally, can the formation of surfaces of discontinuity inside the fluid take place. The analogy to elastic phenomena in solid bodies is easily perceived. In elastic bodies it is the displacements that are the criterions of continuity. In fluid bodies it is the speed gradients. In a solid body if two of its particles are caused to separate a certain distance from each other the body breaks at the point considered. In a fluid body two particles can be separated to any distance inside the fluid mass without destroying the fluid continuity if only the displacement is made without exceeding in the fluid mass certain values of the velocity gradient. But, if in the course of such a displacement too high values of the velocity gradient are reached, the separation of the fluid particles will take place. In other words, in the same way as critical values of displacement bring the breakage of solid bodies, in a similar way critical values of velocity gradient bring fluid breakage. We do not have to do here with fluid breakage in the literal sense of the word, because as soon as the velocity gradient drops below its critical value the fluid particles, if in contact, will rebuild a continuous mass; so that we have to do merely with fluid separation. We are thus brought to an understanding of the phenomenon of fluid separation, it being a question of the velocity gradient.

¹ Washington, D. C., 1919, National Advisory Committee for Aeronautics, Report No. 28.

As soon as the foregoing conception has been reached and we wish to include these phenomena in the domain of dynamics; that is, to apply the concept of *force* to the analysis of these facts, we are immediately brought to the necessity of considering the stress distribution inside the fluid, which stress must depend only on the distribution of the velocity gradient.

The whole question appears as follows: A continuous mass of fluid must be considered as remaining continuous only if, in addition to the equation of continuity being satisfied, the stresses inside the fluid mass do not exceed certain critical values. These critical stresses depend on the distribution of the velocity gradient inside the fluid. When the critical stress is once reached, the fluid mass must disintegrate—that is, surfaces of discontinuity must be formed. If it is the tension stress that first reaches its critical value, simple division of the fluid will take place. If it is the shearing stress that first reaches its critical value, we can have either a simple gliding of a fluid layer over another or the formation of foam; the last on account of the reciprocal property of shearing stresses, which requires that the critical shearing stresses shall appear simultaneously in two orthogonal directions.

The type of flow that establishes itself in each case is such that the stresses inside the fluid are everywhere lower than their critical values. If the critical value is reached somewhere, the flow type changes in such a way that the stresses drop below the critical values. The stress distribution inside a fluid thus appears, in addition to stability requirements, as a fundamental criterion of the flow type.

Let us now formulate the above conception in a more precise form. I will here give only a general sketch of the problem and consider only the most simple case. It will be assumed that the reader is acquainted with the methods of stress analysis and the equation of motion of viscous fluids. According to Stokes for the case of the motion of a viscous fluid parallel to a plane the stresses developed in an element of a fluid are

$$T_{xy} = \mu \left(\frac{\partial u}{\partial y} + \frac{\partial v}{\partial x} \right)$$

$$N_x = -p + 2\mu \frac{\partial u}{\partial x}$$

$$N_y = -p - 2\mu \frac{\partial v}{\partial x}$$

Where N_x and N_y are the normal components of the resultant stress in the surface elements normal to the X and Y axes, and T_{xy} is the tangential component of the resultant stress in the same elements, equal for both elements as result of the reciprocal property of the shearing stresses; p is the pressure at the point considered and μ the viscosity coefficient. We will consider the fluid as incompressible; that is,

$$\frac{\partial u}{\partial x} + \frac{\partial v}{\partial y} = 0$$

and the motion as steady; that is,

$$\frac{du}{dt} = u \frac{\partial u}{\partial x} + v \frac{\partial u}{\partial y}$$

$$\frac{dv}{dt} = u \frac{\partial v}{\partial x} + v \frac{\partial v}{\partial y}$$

The vortex intensity ω at the point considered is given by

$$2\omega = \frac{\partial v}{\partial x} - \frac{\partial u}{\partial y}$$

Let us refer the motion of the fluid at the point considered to what I call the natural fluid coordinates τ and ν whose axes are directed along the tangent to the streamline through the point considered and the principal normal to the same streamline at the same point.

If we designate by V the value of the speed of the fluid particle at the point considered and by V_τ and V_ν the components of V along the τ and ν axes, we find

$$u = V_\tau = V$$

$$v = V_\nu = 0$$

and

$$2\omega = \frac{\partial V_\nu}{\partial \tau} - \frac{\partial V_\tau}{\partial \nu}$$

It is easy to prove that¹

$$\frac{\partial V_\nu}{\partial \tau} = \frac{V}{\rho}$$

and thus

$$\frac{\partial V_\tau}{\partial \nu} = \frac{V}{\rho} - 2\omega$$

Accordingly,

$$\frac{\partial u}{\partial y} + \frac{\partial v}{\partial x} = \frac{\partial V_\tau}{\partial \nu} + \frac{\partial V_\nu}{\partial \tau} = 2\left(\frac{V}{\rho} - \omega\right)$$

And consequently for the tangential stress we find

$$T_{\tau\nu} = 2\mu\left(\frac{V}{\rho} - \omega\right)$$

On the other hand,

$$\frac{du}{dt} = u \frac{\partial u}{\partial x} = V \frac{\partial V}{\partial \tau} = \frac{dV}{dt}$$

on account of $v = V_\nu = 0$; and thus

$$\frac{\partial u}{\partial x} = -\frac{\partial v}{\partial y} = \frac{1}{V} \frac{dV}{dt}$$

and consequently for the normal stresses we find:

$$N_\tau = -p + \frac{2\mu}{V} \frac{dV}{dt}$$

$$N_\nu = -p - \frac{2\mu}{V} \frac{dV}{dt}$$

We thus see that the principal stress axes are making with the τ , ν axes an angle α given by

$$\tan 2\alpha = \frac{V\left(\frac{V}{\rho} - \omega\right)}{\frac{dV}{dt}}$$

The maximum shearing stress is equal to

$$T = 2\mu \sqrt{\left(\frac{V}{\rho} - \omega\right)^2 + \frac{1}{V^2} \left(\frac{dV}{dt}\right)^2}$$

And the principal normal stresses are equal to

$$N_1 = -p + T$$

$$N_2 = -p - T$$

¹ See the papers of Dr. George de Bothezat, edited by the National Advisory Committee for Aeronautics, *General Theory of Blade Screws*, p. 86, or *Introduction into the Study of Laws of Air-resistance of Aerofoils*, p. 61.

The maximum shearing stress T thus appears to depend on the actual speed V of the fluid element considered, the radius ρ of the curvature of its path, its actual tangential acceleration dV/dt and the vortex intensity ω at the point considered. When $(V/\rho - \omega) = 0$ the principal stress axes coincide with the (τ, ν) axes; when $dV/dt = 0$ the principal stress axes bisect the (τ, ν) axes. In the general case the principal stress axes can have any position relative to the (τ, ν) axes.

Discontinuity will appear in the fluid motion if T or N_1 exceed certain critical values. For N_1 the critical value is very close to $N_1 = 0$ or $T = \rho$. If it is T that first reaches a critical value T_c this will give rise to a shearing discontinuity. We will have the formation of surfaces or volumes of discontinuity. But the last as generally admitted are unstable, and will pass over into certain systems of vortices, which can, as seen from the foregoing formulae, release the stresses.

When the expressions for stresses are used at their critical values the viscosity coefficient can not be considered as constant and must take a special critical value at the moment the stresses reach their critical values.

If we designate by σ the cross section of a flow hole, it will be easy to see that

$$\frac{\partial V}{\partial \tau} = -V \frac{d\sigma}{\sigma d\tau}$$

and as

$$\frac{dV}{dt} = V \frac{\partial V}{\partial \tau}$$

we find

$$\frac{dV}{dt} = -V^2 \frac{d\sigma}{\sigma d\tau}$$

and introducing the last value in the expression of the maximum shearing stress we find

$$T = \frac{2\mu V}{\rho} \sqrt{\left(1 - \frac{\rho\omega}{V}\right)^2 + \rho^2 \left(\frac{d\sigma}{\sigma d\tau}\right)^2}$$

The last relation gives the expression of the maximum shearing stress in function of V , ω and the geometrical configuration of the flow.

Karman, at the end of his investigations on the mechanics of fluid resistance,¹ mentions the great importance that the determination by theory of all elements of the vortex systems he studies would have. It is only by the study of the stress distribution inside fluids that the answer to those questions can be found. In the study of lubricating oils, the conception of the critical shearing stress is also of first importance and constitutes the most important property of the oil as lubricating agent.

The determination of the values of the critical stress inside fluids constitutes an experimental problem of first importance.

In the flow experiments of Fales and Caldwell, when we observe the change of the type of flow, which can be seen in a very clear way by the "dew-point" method, as I myself have several times witnessed, this means that the critical stresses have been reached and the flow goes to another type, with another vortex distribution, which releases the stresses.

All the foregoing is only a very short sketch containing merely the statement of the question of a very broad and quite new domain of hydrodynamics. I hope to have some day the opportunity of publishing all the results to which I have been brought in the study of these questions.

DR. GEORGE DE BOTHEZAT.

DAYTON, OHIO, October, 1919.

¹ The paper of Karman's here referred to is given translated as Note IV at the end of Dr. de Bothezat's Introduction to the Study of Laws of Air Resistance of Aerofoils. (See p. 75.)

NOTE II.

THE EFFICIENCY OF A WIND TUNNEL.

By Dr. GEORGE DE BOTHEZAT.

So far as I know no definition of the efficiency of a wind tunnel has been given. The ratios used by different authors for the comparative appreciation of different wind tunnels were purely conventional estimates of the degree of perfection. The whole difficulty resides here in the fact that for a wind tunnel it is not the *engine efficiency* that is involved but the *efficiency of an irreversible cycle*. I will first illustrate by an example exactly what I mean.

Let us consider a rubber ball that undergoes the following cycle: The ball is dropped from a height H_0 with an initial speed equal to zero. At the level H the ball reaches the ground with a speed v , rebounds and rises again. On account of different resistances the ball will not generally reach the original height H_0 . To enable the ball to do so, let us suppose that at the height H_1 , when the ball has the speed v_1 , an impulse is given to it that brings it to such a height H_2 with a speed v_2 , that the ball can afterwards reach its original height H_0 and from there start falling over again. In this example the ball undergoes an irreversible cycle which consists in dropping from a height H_0 , getting a certain kinetic energy equal to $\frac{1}{2}mv^2$, and reaching again the height H_0 by aid of the work done by the impulse.

When the ball drops, its potential energy measured by the height H_0 goes over into kinetic energy. When the ball reaches the level H , its kinetic energy $\frac{1}{2}mv^2$ will generally be less than the work $(H_0 - H)mg$ done by gravity, on account of possible resistances. When the ball rises its kinetic energy goes into potential energy. The work Π equal to

$$\Pi = \frac{1}{2}m(v_2^2 - v_1^2) + (H_2 - H_1)mg$$

represents the work absorbed by the resistances, which has to be communicated to the ball to allow it to reach its original height H_0 .

Thus, in the irreversible cycle considered, the energy put into play is equal to $L = \frac{1}{2}mv^2$. The losses are

$$\Pi = \frac{1}{2}m(v_2^2 - v_1^2) + (H_2 - H_1)mg.$$

The losses expressed in per cent of the energy put into play are equal to

$$\frac{\Pi}{L}.$$

And the efficiency η of our irreversible cycle comes out equal to

$$\eta = 1 - \frac{\Pi}{L} = 1 - \frac{\frac{1}{2}m(v_2^2 - v_1^2) + (H_2 - H_1)mg}{\frac{1}{2}mv^2}$$

If in the fall we had no losses, we would have

$$\frac{1}{2}mv^2 = (H_0 - H)mg.$$

If in addition we assume $v_2 = v_1$ and introduce the notations

$$H_0 - H = h_0; \quad H_2 - H_1 = h_0 - h$$

we find

$$\eta = \frac{h}{h_0}.$$

The foregoing examples presents a complete analogy to the phenomena that take place in a wind tunnel. Let us consider a wind tunnel having an open circuit and fitted with a cone, at

the end of which is disposed a suction fan. The outside air has a pressure p_0 —analogous to the height H_0 of our ball—and a speed zero. The air is sucked into the wind tunnel and in the throat we have a pressure p —analogous to the ground level height H —and an airspeed v . In the cone the air stream expands. The pressure increases and the speed drops. And just in front of the fan we have a pressure p_1 —analogous to the height H_1 —and a speed v_1 . The fan sucks the air and brings it, immediately behind the fan, to a pressure $p_2 > p_1$ and a speed v_2 generally very close to v_1 . Finally by diffusion of the air stream, behind the fan, into the free atmosphere, the airspeed v_2 is lost and the pressure p_0 is reached again. We thus see that the air in the wind tunnel undergoes an irreversible cycle which consists in taking the air at the pressure p_0 , bringing it to the pressure p and speed v and then back again to the pressure p_0 , the losses being compensated by the fan. The energy put into play in this case is equal to

$$L = \Sigma \frac{1}{2} \delta \Delta S v^3.$$

Where ΔS is an annulus of the throat cross section, δ is the density of the air and the sum Σ is taken over the whole throat cross section. If we designate by ΔB the drop in the value of the Bernoulli constant just up to the front of the fan and by ΔB^1 the drop behind, the losses in the wind tunnel flow phenomena come out equal to

$$\Pi = \Sigma \Delta S_1 v_1 (\Delta B + \Delta B^1) + \Sigma \frac{1}{2} \delta_1 \Delta S_1 v_1^3.$$

And the efficiency of the wind tunnel considered, comes out equal to

$$\eta = \frac{L - \Pi}{L} = 1 - \frac{\Sigma \Delta S_1 v_1 (\Delta B + \Delta B^1) + \Sigma \frac{1}{2} \delta_1 \Delta S_1 v_1^3}{\Sigma \frac{1}{2} \delta \Delta S v^3}.$$

Let us take the ideal case of a wind tunnel for which $\Delta B + \Delta B^1 = 0$. For such a case we will find

$$\eta = 1 - \frac{\frac{1}{2} \Sigma \delta_1 \Delta S_1 v_1^3}{\frac{1}{2} \Sigma \delta \Delta S v^3}$$

If in addition we assume v and v_1 constant in the corresponding cross-sections, then, on account of flow continuity, expressed by $\delta_1 \Delta S_1 v_1 = \delta \Delta S v$, we find

$$\eta = 1 - \frac{v_1^2}{v^2} = 1 - \frac{\delta^2 S^2}{\delta_1^2 S_1^2}$$

The values of δ and δ_1 can be calculated to a first approximation by assuming the whole process to be adiabatic. The last expression represents thus the efficiency of an ideal wind tunnel, that is, the limit that a real wind tunnel can not reach.

In some wind tunnels the losses Π are so great that $\Pi > L$, then the efficiency comes out negative; this only means that the wind tunnel considered is so poor that the losses exceed the energy put into play.

Let us now designate by ρ the efficiency of the fan and by L_m the power output of the motor that drives the fan. We will then have

$$\Pi = \rho L_m$$

The efficiency of the wind tunnel then becomes

$$\eta = 1 - \frac{\rho L_m}{L}$$

The total efficiency of the wind-tunnel-fan system is equal to

$$\eta^1 = \frac{L - L_m}{L} = 1 - \frac{\Pi}{\rho L}$$

If we designate by Δp the pressure difference that the fan maintains on its two sides, the useful work done by the fan comes out equal to

$$\Sigma \Delta p \Delta S_1 v_1 = \Sigma \Delta S_1 v_1 (\Delta B + \Delta B^1) + \Sigma \frac{1}{2} \delta \Delta S_1 v_1^3 = \Pi$$

thus

$$\Delta p = (\Delta B + \Delta B^1) + \frac{1}{2} \delta v_1^2$$

considering

$$v_1 \cong v_2$$

I will remark here that the main part of the losses in a wind tunnel are made up of the losses in the cone and the kinetic energy of the air leaving the wind tunnel. For the whole wind-tunnel-fan system the fan losses have to be added.

One of the most delicate parts of the wind tunnel problem is the phenomenon of the flow expansion in the cone. The author of this note is of the opinion that if the fluid were ideal, no expansion could take place, and that the expansion obtained in wind tunnel cones is exclusively due to fluid viscosity. This brings us to think that improvement of wind tunnels could be reached by providing some special arrangements in the cone, which would oblige the stream to expand.

The foregoing can easily be extended to wind tunnels with closed circuit.

This short note has to be considered only as a short sketch of the question of the wind-tunnel efficiency, which gives merely the conceptional part of the problem. The author hopes to have some day the opportunity to treat more completely the wind tunnel problem.

Dr. GEORGE DE BOTHEZAT.

DAYTON, OHIO, October, 1919.

